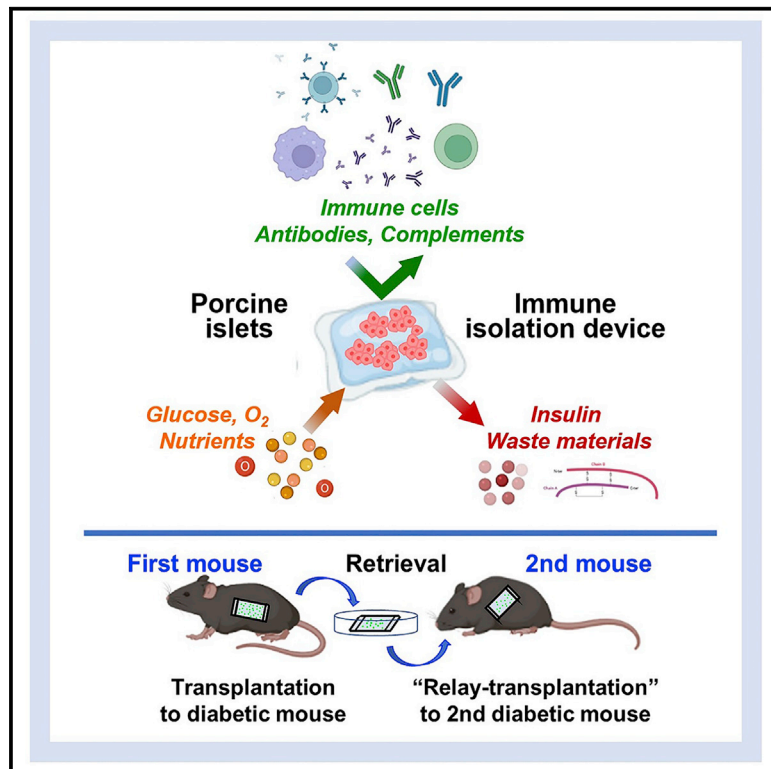


A porcine islet-encapsulation device that enables long-term discordant xenotransplantation in immunocompetent diabetic mice

Graphical abstract



Authors

Kumiko Ajima, Naoto Tsuda, Tadashi Takaki, ..., Sayaka Amano, Chinatsu Oyama, Masayuki Shimoda

Correspondence

mshimoda@hosp.ncgm.go.jp

In brief

Ajima et al. develop a maintenance-free, replaceable porcine islet-encapsulating device to secrete insulin in response to hyperglycemia. Stability, permeability, biocompatibility, and immunoisolation were achieved by using a crosslinked hydrogel and a semipermeable membrane. Discordant xenotransplantation of the device into diabetic mice improved glycemic control without immunosuppressants.

Highlights

- Design of a porcine islet encapsulation macrodevice to serve as a bioartificial pancreas
- The device utilizes alginate gel and an immunoprotective membrane
- The device prevents rejection during sequential xenotransplantations
- Stability, permeability, biocompatibility, and immunoisolation are demonstrated



Article

A porcine islet-encapsulation device that enables long-term discordant xenotransplantation in immunocompetent diabetic mice

Kumiko Ajima,¹ Naoto Tsuda,² Tadashi Takaki,^{1,3,4} Shoji Furusako,⁵ Shigeki Matsumoto,² Koya Shinohara,¹ Yzumi Yamashita,¹ Sayaka Amano,¹ Chinatsu Oyama,⁶ and Masayuki Shimoda^{1,7,*}

¹Pancreatic Islet Cell Transplantation Project, Research Institute National Center for Global Health and Medicine, 1-21-1 Toyama Shinjuku-ku, Tokyo 162-8655, Japan

²Biomaterials Business Division, Mochida Pharmaceutical Co., Ltd., 722 Uenohara, Jimba, Gotemba, Shizuoka 412-8524, Japan

³Department of Cell Growth and Differentiation, Center for iPS Cell Research and Application, Kyoto University, 53 Kawahara-cho, Shogoin, Sakyo-ku, Kyoto 606-8507, Japan

⁴Takeda-CiRA Joint Program (T-CiRA), 2-26-1 Muraoka-higashi, Fujisawa-shi, Kanagawa 251-8555, Japan

⁵Biomaterials Business Division, Mochida Pharmaceutical Co., Ltd., 1-7 Yotsuya, Shinjuku-ku, Tokyo 160-8515, Japan

⁶Communal Laboratory, Research Institute National Center for Global Health and Medicine, 1-21-1 Toyama, Shinjuku-ku, Tokyo 162-8655, Japan

⁷Lead contact

*Correspondence: mshimoda@hosp.ncgm.go.jp

<https://doi.org/10.1016/j.crmeth.2022.100370>

MOTIVATION A shortage of donors and the need for immunosuppressants are major issues of islet transplantation for the treatment of type 1 diabetes (T1D). Therefore, we are developing T1D treatment using xenogeneic islets and bioartificial pancreas (BAP). However, no BAP devices currently meet all of the functions of long-term glycemic control, islet survival, immunoprotection, discordant xenotransplantation feasibility, and biocompatibility. To address this, we developed a hydrogel with long-term stability and permeability for encapsulating islets in this study. Furthermore, we found an immunoprotective membrane with high biocompatibility for wrapping xenogeneic islets and used them to develop BAP devices.

SUMMARY

Islet transplantation is an effective treatment for type 1 diabetes (T1D). However, a shortage of donors and the need for immunosuppressants are major issues. The ideal solution is to develop a source of insulin-secreting cells and an immunoprotective method. No bioartificial pancreas (BAP) devices currently meet all of the functions of long-term glycemic control, islet survival, immunoprotection, discordant xenotransplantation feasibility, and biocompatibility. We developed a device in which porcine islets were encapsulated in a highly stable and permeable hydrogel and a biocompatible immunoisolation membrane. Discordant xenotransplantation of the device into diabetic mice improved glycemic control for more than 200 days. Glycemic control was also improved in new diabetic mice “relay-transplanted” with the device after its retrieval. The easily retrieved devices exhibited almost no adhesion or fibrosis and showed sustained insulin secretion even after the two xenotransplantations. This device has the potential to be a useful BAP for T1D.

INTRODUCTION

Islet transplantation is an attractive therapy for unstable patients with type 1 diabetes (T1D).^{1–3} However, donor shortage is a major problem, in addition to the continuous use of immunosuppressants. Islet xenotransplantation using porcine islets is drawing attention as a means to overcome the donor shortage. In clinical trials involving the transplantation of neonatal porcine islets into diabetic patients in Sweden, serum porcine C-peptide was

detected and graft survival was confirmed.⁴ Furthermore, in clinical trials in New Zealand and Argentina, the glycemic control of patients with T1D improved after they were transplanted with alginate microcapsules encapsulating neonatal porcine islets.^{5,6}

Pigs are an advantageous source for islet cells because they have high fertility and because a large amount of islets can be acquired at low cost. In addition, in contrast to human cadaver donors, there would be minimal damage to the tissue due to ischemia or lethal diseases, and quality-controlled and fresh



organs and cells can be obtained. There is no concern about tumorigenicity, which is a problem with embryonic stem cells and induced pluripotent stem-derived cells.⁷ In addition, pig-to-human infectious diseases can be controlled by using pathogen-free pigs. Although infection of the porcine genome by porcine endogenous retrovirus (PERV) is a concern, PERV infection has not yet been observed in humans in multiple clinical studies.^{8–10} However, innate immune reactions, acquired immune reactions,^{11,12} and sustained inflammatory effects¹³ occur in porcine islet xenotransplantation, and therefore administration of multiple immunosuppressants is required.¹⁴

Accordingly, encapsulation of islets in a special capsule capable of immunoisolation, known as a bioartificial pancreas (BAP), is a promising method for protecting islets from rejection and inflammatory responses.^{15,16} Microcapsule BAPs using a polymer gel have achieved positive results in clinical studies, including a reduction in the required insulin amount and a decrease in HbA1c levels and hypoglycemia unawareness.^{17–19} However, there are problems, such as insufficient immunoisolation ability, degradation of the capsules, and difficulty in the complete retrieval of the capsules. To address these problems, large-sized macrodevice BAPs with robust mechanical strength have been developed in recent years.^{15,16} β Air,^{20–22} developed by β O₂ Technologies, is a Teflon membrane chamber with a port for oxygen supply that is embedded in a multilayered structure of alginate gel containing human islets. Subcutaneously transplanted β Air devices have achieved insulin secretion for 10 months. However, β Air requires daily oxygen supplementation. ViaCyte is conducting clinical trials (NCT04678557, NCT02239354) involving subcutaneous transplantation of semipermeable devices called PEC-Encap that contain human embryonic stem cell-derived pancreatic progenitor cells.^{23–25} Nonetheless, problems have been found with the supply of oxygen and nutrients to the cells and with the biocompatibility of the device. Currently in clinical trials (NCT03163511), PEC-Direct is a direct vascularization device that unfortunately requires the use of immunosuppressants.²⁶ In addition, new macrodevices that promote angiogenesis have been developed, including Sernova's Cell Pouch^{27,28} and Defymed's MailPan.²⁹ However, clinical trials of macrodevices have not yet reported excellent long-term transplantation results, even with allogeneic transplantation. Cell engraftment by macrodevices is even more difficult in xenotransplantation than in allogeneic transplantation. Necessary improvements include more appropriate biocompatible materials with sufficient supplies of oxygen and nutrients, maintenance of secretory insulin permeability for rapid glycemic control, the maintenance of isolation from the host's immune system, and the ability to suppress the inflammatory response.³⁰

Here, we created a BAP device by encapsulating adult porcine islets in a developed alginate gel with excellent permeability and stability and then enclosing them in a highly biocompatible semipermeable membrane bag with immunoisolation capability. The transplantation of these devices into the abdominal cavities of immunocompetent wild-type diabetic mice without the use of any immunosuppressant led to a clear and rapid lowering of blood glucose and long-term glycemic control and survival of porcine islets. One of its main advantages is that it can be easily retrieved with almost no adhesion, even after long-term transplantation. Furthermore, the devices still functioned after their

retrieval from the first transplanted mice and their relay-transplantation into new immunocompetent wild-type diabetic mice. This is the first report of such a device that still functioned after two transplants and that therefore withstood discordant xenogeneic biological reactions twice.

RESULTS

Device fabrication

Figure 1A shows the appearance of the fabricated transplantation device. It is a semipermeable membrane bag (10 × 24 mm), and both ends are heat sealed (size without seal: 10 × 20 mm). An alginate gel encapsulating porcine islets is enclosed in the bag (Figure 1A). The molecular weight cut-off for the semipermeable membrane is 100 kDa. Figure 1B shows a schematic of the device production and transplantation. The porcine pancreas was extracted and digested by collagenase. The porcine islets were dispersed in a sodium alginate solution and encapsulated in a semipermeable membrane bag. The devices were intraperitoneally transplanted into immunocompetent diabetic mice not being administered immunosuppressants. Figure 1C shows the chemical structural formulas of both natural and chemically modified sodium alginate.

Alginate gel stability *in vitro*

In stability tests (Figure 2A), the Ca²⁺ crosslinked 50 μ L-0.5% natural alginate gel (NAG) was shaken in physiological saline. Almost all alginate was eluted after 1 h. In the Ca²⁺ crosslinked 200 μ L-1.0% NAG, approximately 35% of the alginate was dissolved after 5 h shaking (Figure 2A). Although the dissolution rate was lower for thicker gels, a significant amount of NAG still dissolved. In contrast, the 50 μ L-0.5% chemically crosslinked alginate gel (CCAG) did not disintegrate even after 96 h (Figure 2A). Thus, the CCAG had much better gel stability than the NAG.

Glucose, insulin, and IgG permeability *in vitro*

In permeability testing of glucose and insulin in the semipermeable membrane alone, both molecules showed good permeability (Figures 2B and 2C). In permeability testing of the device (semipermeable membrane + alginate gel), the thinner the gel, the faster the transmission speed (Figure 2D). For insulin, approximately 80% of human insulin permeated within 4 h in both NAGs and CCAGs (Figure 2E). For IgG, both the NAG and CCAG devices did not pass most of the IgG-FITC (Figure 2F).

Complement permeability

A sensitized sheep erythrocyte hemolysis test was performed to examine the permeability of complement in the semipermeable membrane or in various alginate gels. Although the hemolysis rate of sensitized sheep erythrocytes was about 10% in all gels (Figure 2G, green and blue), the rate was almost 0% in the semipermeable membranes (Figure 2G, gray). The device can thus prevent the reaction of complement against the inner cells.

Simulation of device thickness, inner oxygen concentration, and insulin secretion

A simulation was performed of the oxygen concentration in the device, under the condition in which the device was in the

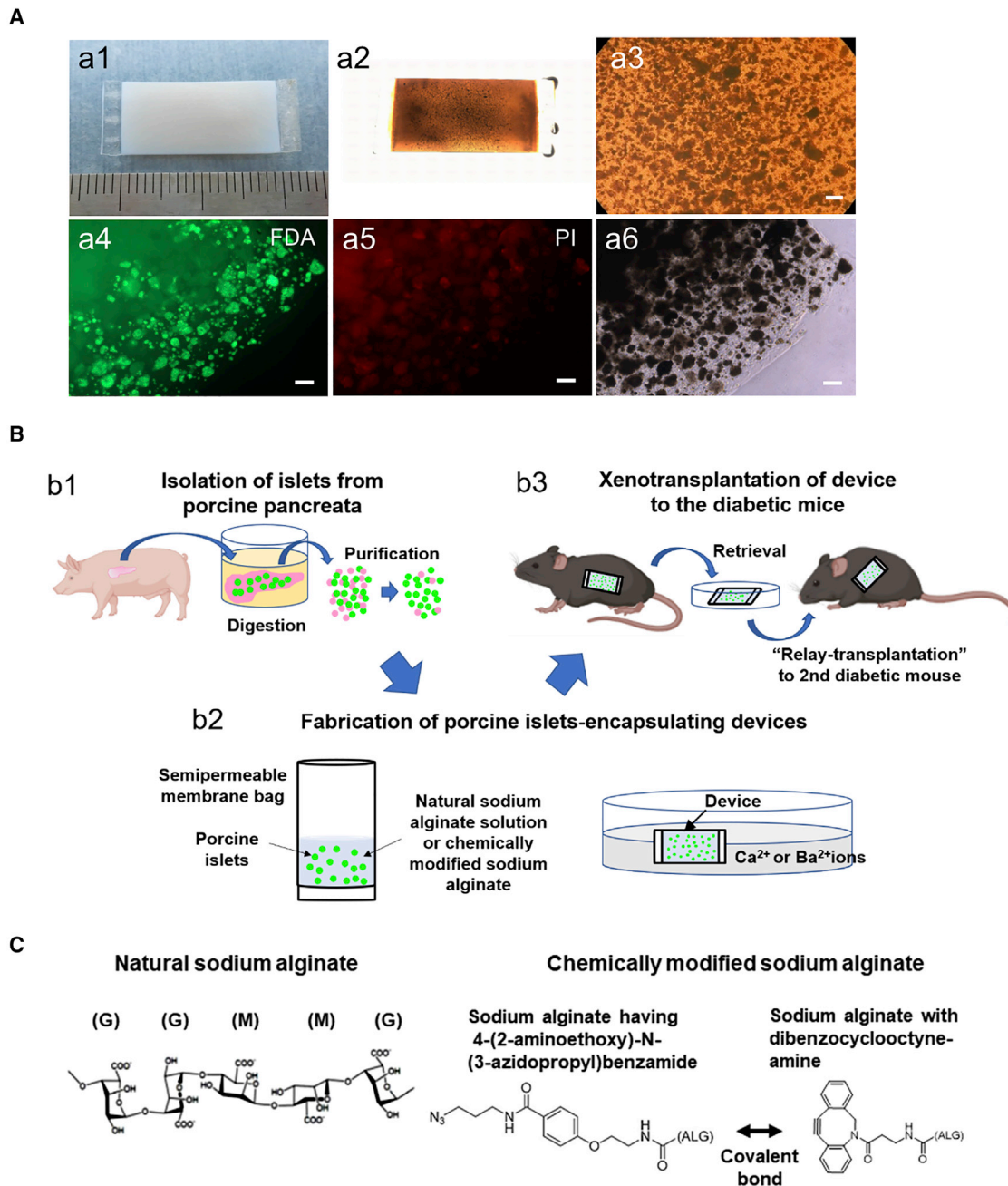


Figure 1. Device production and transplantation into immunocompetent wild-type diabetic mice followed by relay-transplantation into a second diabetic mouse

(A) Device comprising alginate gel encapsulating porcine islets in a semipermeable membrane (panel 1). Optical microscopic image of the device showing porcine islets dispersed in the alginate gel (panels 2 and 3). Porcine islets encapsulated in alginate gel stained with FDA in a device before transplantation (panel 4). Porcine islets encapsulated in alginate gel stained with propidium iodide in a device before transplantation. The porcine islets of the pre-transplant devices were confirmed to survive in the alginate gel (panel 5). Bright-field image of porcine islets encapsulated in alginate gel. The sodium alginate in the device was gelled into a sheet shape (panel 6). Scale bar, 200 μm .

(B) The porcine pancreas was extracted from adult pigs and digested by collagenase solution. Porcine islets mixed with exocrine cells were purified according to specific density (panel 1). The porcine islets were dispersed in either a natural sodium alginate solution or a chemically modified sodium alginate solution. By immersing the device in a solution of calcium or barium ions to gel the sodium alginate, the porcine islets were encapsulated in the alginate gel in a semipermeable membrane bag (panel 2). Devices comprising alginate gel encapsulating porcine islets were intraperitoneally transplanted into immunocompetent diabetic mice not being administered immunosuppressants (panel 3).

(C) Chemical structural formulas of both natural and chemically modified sodium alginate. Sodium alginate with 4-(2-aminoethoxy)-N-(3-azidopropyl) benzamide and sodium alginate with dibenzocyclooctyne-amine were covalently bonded to form chemically crosslinked alginate acid.

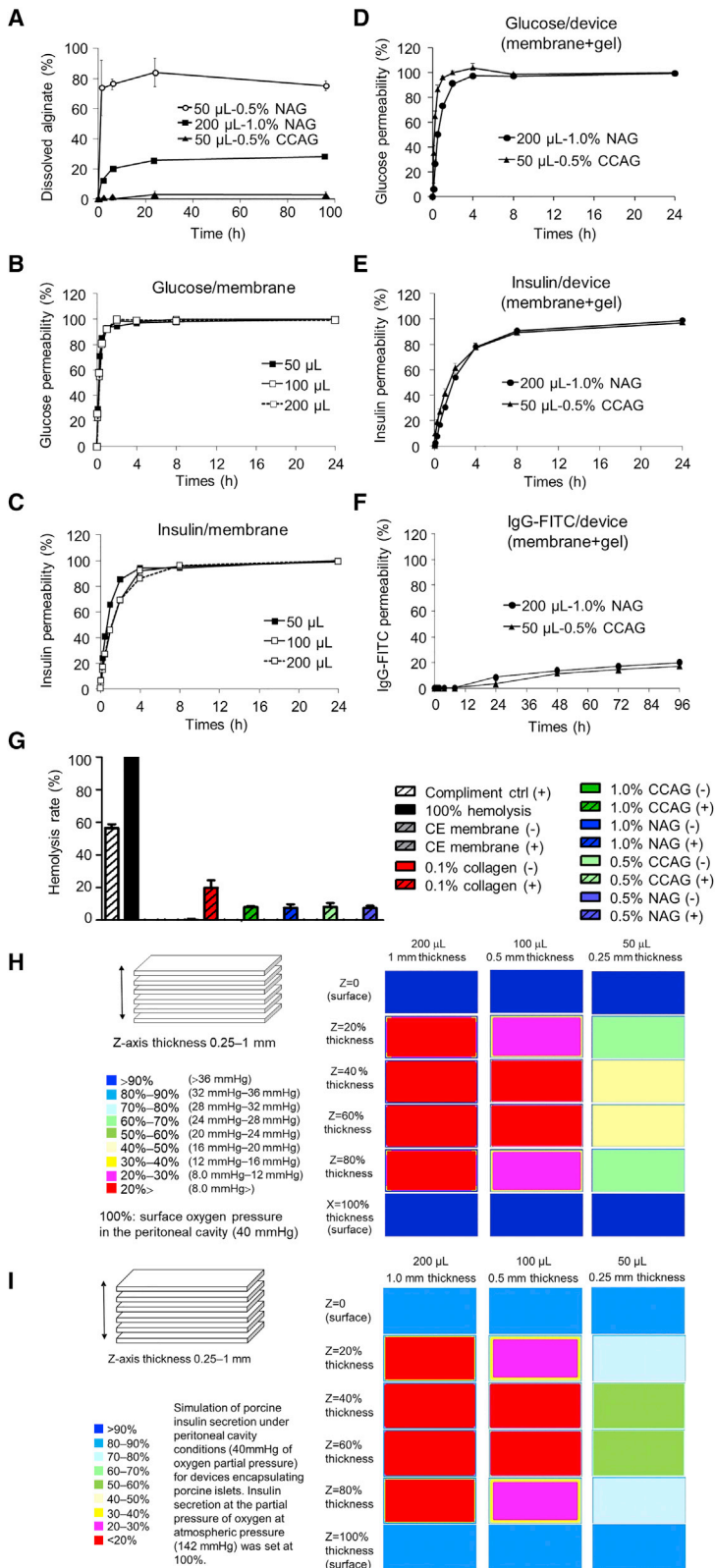


Figure 2. Stability and permeability of gel/device

(A) Gel stability of the NAG and CCAG. The NAG sheet decomposed within 1 h, whereas the CCAG sheet was stable with no decomposition.

(B) Glucose permeated the semipermeable membrane bag to almost 100% within 1 h.

(C) Insulin permeated the semipermeable membrane bag to 100% in 4 h.

(D) Glucose passed through the device in 4 h.

(E) Up to 80% of the insulin passed through the device in 4 h.

(F) IgG permeability. A semipermeable membrane device containing the 200 μ L-1.0% NAG device or the 50 μ L-0.5% CCAG device retained most of the IgG-FITC in the device.

(G) Complement isolation. The hemolysis rate of erythrocytes in the semipermeable membrane bag was 0% (gray). In the case of alginate gel containing erythrocytes, the hemolysis rate of erythrocytes was about 10% in both the NAG and CCAG (green and blue).

(H) Simulation of the oxygen permeability of the porcine islet-encapsulating device. The oxygen concentration in the device was simulated for each cross-section of the device in the z axis. For devices containing 50- μ L alginate gel, the oxygen concentration of the gel near the surface exceeded 90% (blue), whereas that of the gel in the device center was 40%–50% (light yellow).

(I) Simulations were performed to predict the percentage of insulin secretion from porcine islets inside the device when the insulin secretion at the partial pressure of oxygen at atmospheric pressure (142 mmHg) was set to 100%. The partial pressure of oxygen inside the abdominal cavity, that is, the partial pressure of oxygen at the device surface layer, was set to 40 mmHg. The 50- μ L alginate gel device maintained more than 50% (green) insulin secretion, even in the central region.

intraperitoneal cavity and the encapsulated islet cells consumed oxygen. The oxygen concentration in the islet-encapsulating device (semipermeable membrane + alginate gel + porcine islets) was compared for each amount of alginate gel: 200, 100, and 50 μL (gel thickness: 1, 0.5, and 0.25 mm, respectively). The number of islets per volume of these devices was 50, 100, and 200 islet equivalents (IEQ)/ mm^3 , respectively (1 IEQ: standardized diameter of 150 μm).³¹ Assuming an oxygen concentration of 100% outside the device, the oxygen concentration near the surface of the 1-mm alginate gel was 90% or more (Figure 2H, blue). However, the oxygen concentration of the gel center was 20% or less (red). On the other hand, in a thin 0.25-mm alginate gel, the oxygen concentration of the center was maintained at 40%–50% (Figure 2H, light yellow).

Insulin secretion from islets is considered to decrease in a hypoxic environment.³² A simulation was performed of insulin secretory capacity according to the local oxygen pressure based on the thickness of the device encapsulating the islets. Figure 2I shows the simulation of porcine insulin secretion under peritoneal cavity conditions (40 mmHg of partial pressure of oxygen) for devices encapsulating porcine islets, setting insulin secretion at a partial pressure of oxygen at atmospheric conditions (142 mmHg) as 100%. In this case, insulin secretion at the device surface was estimated to be 80%–90% of that at atmospheric pressure, and the internal insulin secretion of the 1-mm alginate gel was less than 20% (Figure 2I, red). On the other hand, 50%–60% insulin secretion of that of atmospheric pressure was maintained, even in the central part of the 0.25-mm alginate gel (Figure 2I, green).

Alginate gel stability *in vivo*

Compared with the gels before transplantation (panels 1 and 2 in Figure 3A), the 200 μL -1.0% NAG dissolved and fragmented after transplantation into the abdominal cavities of the mice for 3 months (panel 3 in Figure 3A, panels 1–3 in Figure 3B). In contrast, the 50 μL -0.5% CCAG maintained its shape without fragmentation (panel 4 in Figure 3B), consistent with the *in vitro* stability test results (Figure 2A).

Mechanical strength of cellulose membranes

Tension test results for a cellulose membrane (35 \times 6 mm) cut into a dumbbell shape are shown in Figure S5. The ultimate tension strengths in the longitudinal and lateral directions were 1.87 and 1.48 N, respectively, while the longitudinal or lateral fracture strains were 6.10 and 7.53 mm, respectively.

Effectiveness of a porcine islet-encapsulating device for xenotransplantation

Figure 3C shows the changes in non-fasting blood glucose levels in immunocompetent wild-type diabetic mice intraperitoneally transplanted with 200 μL -1.0% NAG devices encapsulating porcine islets at 5,000, 10,000, and 12,000 IEQ without the use of any immunosuppressants. Although some mice exhibited an early increase in blood glucose after transplantation, some mice showed improved blood glucose levels for over a year. Of the 30 mice, 3 (10%) showed long-term glycemic control (Table 1). Thus, a long-term improvement in blood glucose was observed using the NAG, although it was still at a low rate. On

the other hand, it was confirmed that some porcine islets were alive in the device retrieved from the mice whose blood glucose level increased 1 week after transplantation (Figure S1), indicating that, even in such mice, not all of the islets in the devices were destroyed. Two of the mice were found to have elevated blood glucose levels after device retrieval, indicating that the transplanted device helped to improve glycemic control. In other mice, no increase in the blood glucose level could be confirmed after retrieval. This may be because endogenous β cells had regenerated over the long study period.^{33,34}

Meanwhile, mice that were not transplanted with the device remained hyperglycemic (Figure S2). From the Kaplan-Meier curve of the percentage of mice with improved blood glucose levels after transplantation with a 200 μL -1.0% NAG device containing 5,000, 10,000, or 12,000 IEQ porcine islets, the percentage of mice with improved blood glucose levels was found to be better with 10,000 or 12,000 IEQ than with 5,000 IEQ (Figure 3D). As shown in the Kaplan-Meier curve in Figure 2D, the percentage of mice with improved blood glucose levels was higher for 10,000 IEQ than for 5,000 IEQ, and there was no difference between 10,000 and 12,000 IEQ. Therefore, in this study, we set the conditions at 10,000 IEQ because this number of porcine islets seemed the most effective for identifying the optimal transplantation device conditions. Next, to examine the optimal conditions for the developed CCAG in this study, long-term glycemic control was compared among diabetic mice transplanted with various devices encapsulating 10,000 IEQ of porcine islets (Table 1). With the minimal gel thickness, the minimal gel concentration, and a low induction rate of chemical crosslinking, the rate was increased to 61.9% (the 50 μL -0.5% CCAG group; Figure 3E), which was significantly higher than that of the 200 μL -1.0% NAG group (Figure 3F). These conditions suggest improved nutrient and oxygen permeability and porcine islet survival. In glucose tolerance testing, the blood glucose levels in mice transplanted with the 200 μL -1.0% NAG device (black circle) and the 50 μL -0.5% CCAG device (black triangle) increased 30 min after glucose administration and decreased to the pre-administration levels 3 h later (Figure 3G). In addition, the serum porcine insulin in mice transplanted with the 0.5% CCAG device was about 1–5 mU/L from 2 to 31 weeks after transplantation (Figure 3H). In an *in vitro* assay, the insulin secretion levels in pre-transplant devices encapsulating 10,000 IEQ porcine islets were approximately 1,000 mU/L (Figure 3I). *In vitro* assays showed that insulin secretion from 0.5% CCAG devices retrieved 178–214 days after transplantation was reduced compared with pre-transplantation, but it was maintained at approximately 60 mU/L (Figures 3I and 3J). From a paired t test, in GSIS testing of the device before transplantation, insulin secretion did not show a significant difference in glucose concentration dependence (Figure 3I), whereas, in GSIS testing of the device after retrieval, insulin secretion showed a significant increase in glucose concentration responsiveness (Figure 3J). Thus, the islets inside the device survived over a long period of time and exhibited glucose responsiveness.

To investigate the biological reaction to porcine islet-encapsulating devices, we examined the devices retrieved over time from the mice. For both the NAG and CCAG devices encapsulating porcine islets, which were wrapped only in a thin, transparent

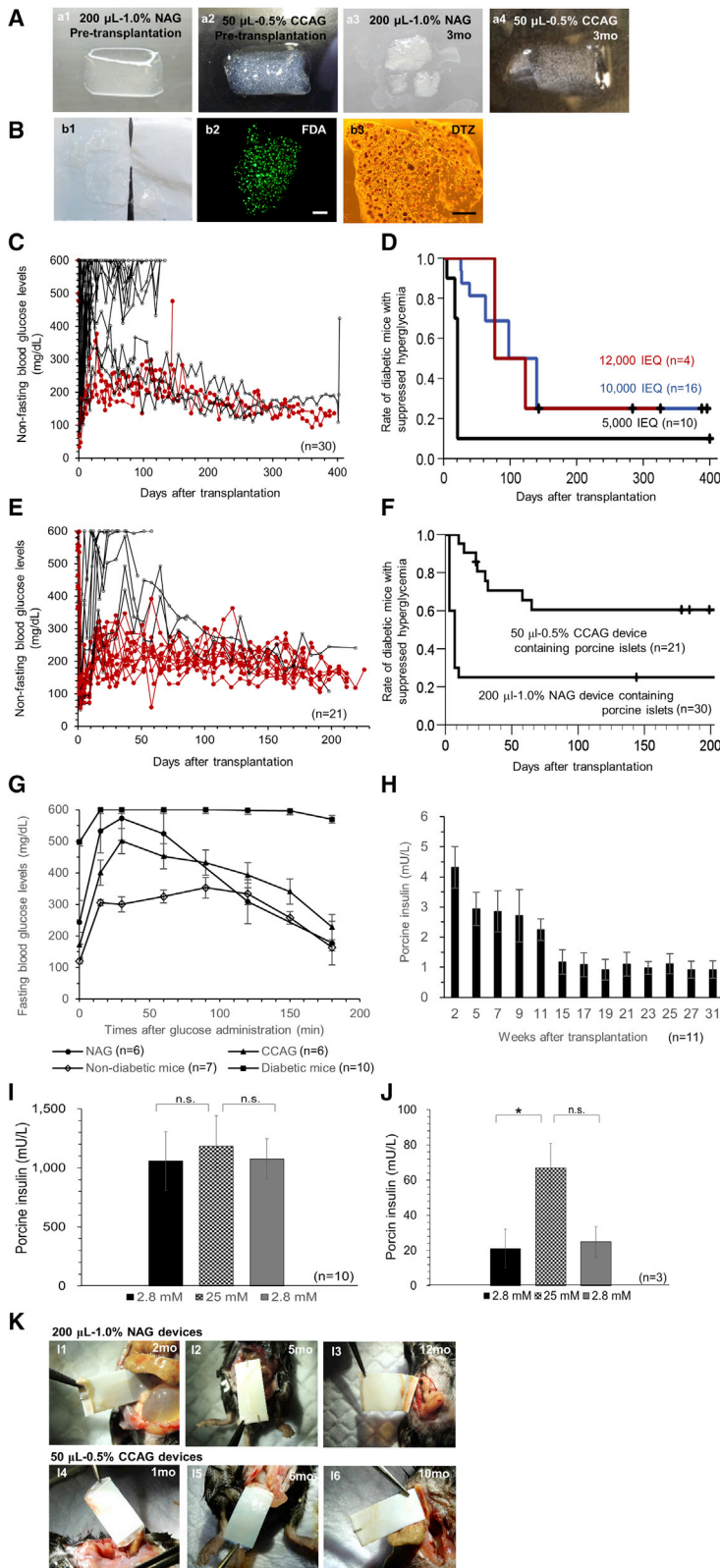


Figure 3. Effectiveness of the devices

(A) Porcine islet-encapsulating alginate gel in pre- and post-transplant devices.

(B) A 200 μ L-1.0% NAG device encapsulating porcine islets retrieved on day 143 after transplantation that still improved blood glucose levels. Scale bar, 1 mm.

(C) Changes in non-fasting blood glucose levels in immunocompetent diabetic mice transplanted with a 200 μ L-1.0% NAG device encapsulating porcine islets.

(D) Kaplan-Meier curve of the percentage of mice with an improved blood glucose level after transplantation with a 200 μ L-1.0% NAG device encapsulating 5,000, 10,000, and 12,000 IEQ of porcine islets (Bonferroni-adjusted $p < 0.017$).

(E) Changes in non-fasting blood glucose levels in immunocompetent wild-type diabetic mice transplanted with 50 μ L-0.5% CCAG devices encapsulating 10,000 IEQ of porcine islets.

(F) Kaplan-Meier curve of the percentage of mice with an improved blood glucose level after transplantation with a 50 μ L-0.5% CCAG device and a 200 μ L-1.0% NAG device encapsulating porcine islets ($p < 0.001$).

(G) Intraperitoneal glucose tolerance test. (H) Non-fasting blood porcine insulin in diabetic mice transplanted with a 0.5% CCAG device encapsulating 10,000 IEQ of porcine islets.

(I) Glucose-stimulated insulin secretion (GSIS) from 50 μ L-0.5% CCAG devices encapsulating 10,000 IEQ of porcine islets before transplantation. Glucose concentration-dependent insulin secretion was compared using a paired t test.

(J) GSIS from 0.5% CCAG devices encapsulating 10,000 IEQ of porcine islets 178–214 days after transplantation. Glucose concentration-dependent insulin secretion was compared using a paired t test.

(K) Devices retrieved from the abdominal cavity of immunocompetent wild-type diabetic mice.

See also [Video S1](#).

Table 1. Effectiveness of glycemic control in diabetic mice

Types of alginate gel used in transplant devices (contains 10,000 IEQ porcine islets)	No. of diabetic mice transplanted with the devices	No. of diabetic mice with improved blood glucose levels	Percentage of diabetic mice with improved blood glucose levels
A 200 μ L-1.0% NAG	30	3	10.0
B 200 μ L-1.0% CCAG (induction rate, 5.0%)	7	0	0.0
C 200 μ L-0.5% CCAG (induction rate, 5.0%)	11	3	27.3
D 100 μ L-0.5% CCAG (induction rate, 5.0%)	7	3	42.9
E 200 μ L-0.5% CCAG (induction rate, 2.3%)	10	4	40.0
F 100 μ L-0.5% CCAG (induction rate, 2.3%)	13	5	38.5
G 50 μ L-0.5% CCAG (induction rate, 2.3%)	21	13	61.9

film, almost no adhesion or notable fibrosis was visible even more than 10 months after transplantation, and they were easily retrieved. No device deformation or damage was observed (Figure 3K; Video S1).

Confirmation of device effectiveness relay-transplanted into a second diabetic mouse

To prove that transplanted 50 μ L-0.5% CCAG devices with porcine islets maintained their function for a long time, they were retrieved at 22–396 days after transplantation and relay-transplanted into other immunocompetent wild-type diabetic mice. Of the 31 transplanted mice, 16 exhibited blood glucose levels below 300 mg/dL for 1 month (Figures 4A, 4B, and S3). From the Kaplan-Meier curve, more than half of the mice improved their blood glucose levels for 1 month (Figure 4C).

About 1 month after transplantation, the relay-transplanted devices were easily retrieved with almost no adhesion or fibrosis, similar to after the first transplantation (Figure 4D). These re-retrieved devices showed insulin secretion *in vitro*, even after the two xenotransplantations (Figure 4E). A paired t test of GSI from the re-retrieved device showed no statistically significant difference due to the small sample size, although it seems that there was a tendency for glucose responsiveness.

Immunohistochemical analysis of the devices

Regarding the hosts' responses to the devices, the devices were retrieved and stained 6 days after transplantation. No host cells were found inside the device, although a single layer of macrophages was evident on the device surface (Figure 5A). T lymphocytes stained with anti-CD3 antibody were also found in a few layers of cells attached to the surface of the device (Figure 5B). Mesothelial cells were in the outermost layer of the thin film formed on the surface of the device 3 months after transplantation (Figure 5C).

At more than 200 days after transplantation, there were some areas where islets in the gel had disappeared compared with the device before transplantation. However, both the 200 μ L-0.5% CCAG and 50 μ L-0.5% CCAG devices encapsulating porcine islets showed many existing porcine islets (panels 1–3 in Figure 5D, panels 1–3 in Figure 5E) that expressed insulin (green) and glucagon (red) (panels 4–6 in Figure 5D, panels 4–6 in Figure 5E). Host-derived mouse IgG was partially observed in the semipermeable membrane and on the surface of the gel (panel 7 in Figure 5D), but was hardly localized around the islets (panel 7 in Figure 5E, panel 7 in Figure 5F). Host-derived mouse C3 did not invade the devices (panel 11 in Figure 5D, panel 11 in Figure 5E, panel 11 in Figure 5F). Figure 5F shows tissue section images of a 200 μ L-0.5% CCAG device encapsulating porcine islets retrieved 26 days after relay-transplantation after the 305-day initial transplantation and Figure 5G shows a 50 μ L-0.5% CCAG device encapsulating porcine islets retrieved on day 41 of relay-transplantation after the 148-day initial transplantation. In both devices, porcine islets survived and expressed insulin and glucagon (panels 1–6 in Figure 5F, panels 1–6 in Figure 5G). Host-derived mouse IgG and C3 did not invade the devices, even after relay-transplantation (panels 7 and 11 in Figure 5G, panels 7 and 11 in Figure 5G).

Electron microscopic analysis of the devices

The surface of the semipermeable membrane was smooth before transplantation and contained numerous holes. The cross-sections of the membrane showed sponge-like structures (panels 1 and 2 in Figure 5H). The surface of a 50 μ L-0.5% CCAG device encapsulating porcine islets transplanted into diabetic mice for 6 months had granular and sparse fibrous deposits but the surface pores were not blocked. No substances were determined to have invaded the sponge-like structure of the semipermeable membrane (panels 3 and 4 in Figure 5H).

DISCUSSION

We developed macrodevices encapsulating porcine islets in a highly stable and permeable alginate gel and biocompatible

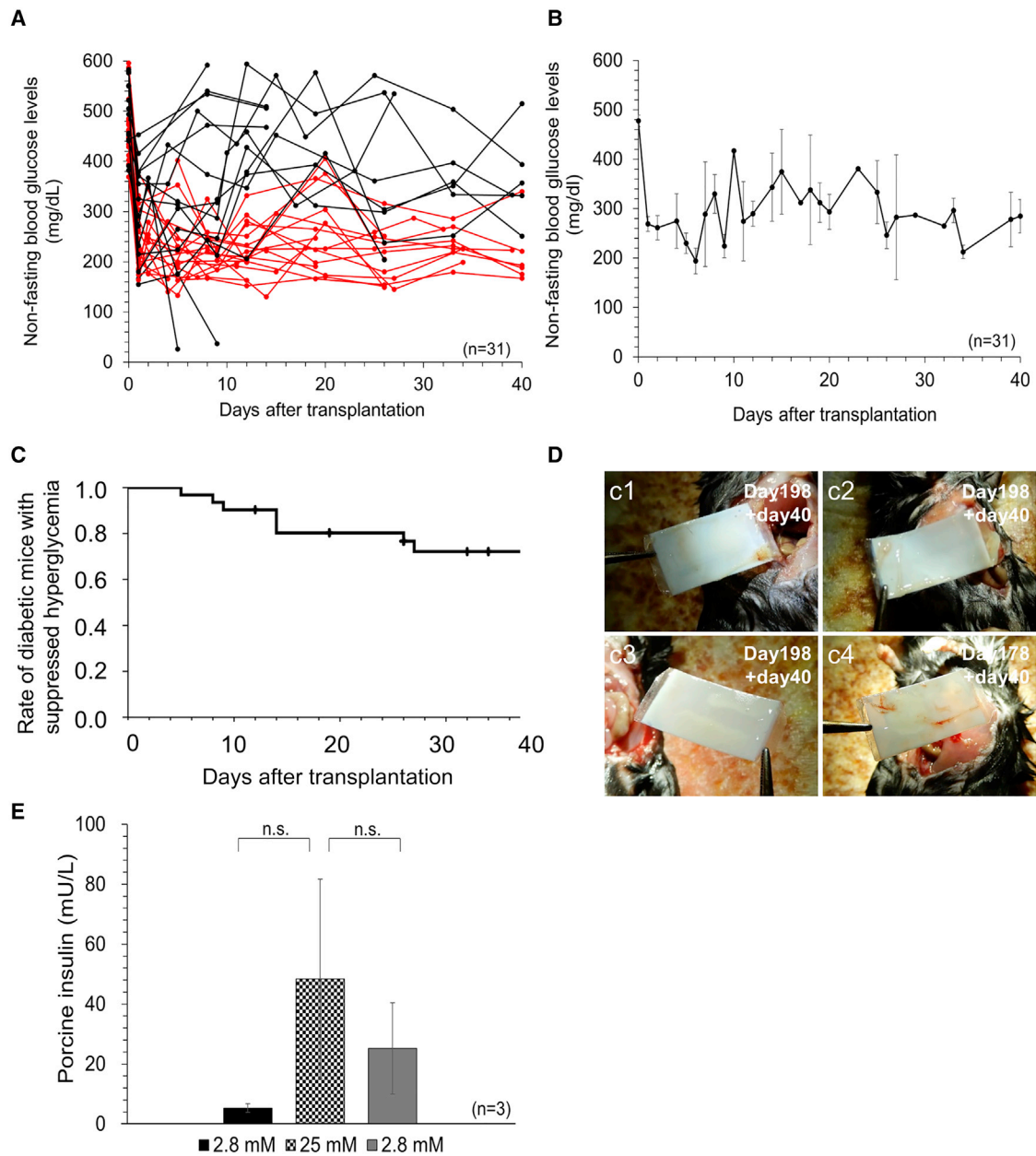


Figure 4. Effectiveness of the relay-transplanted devices

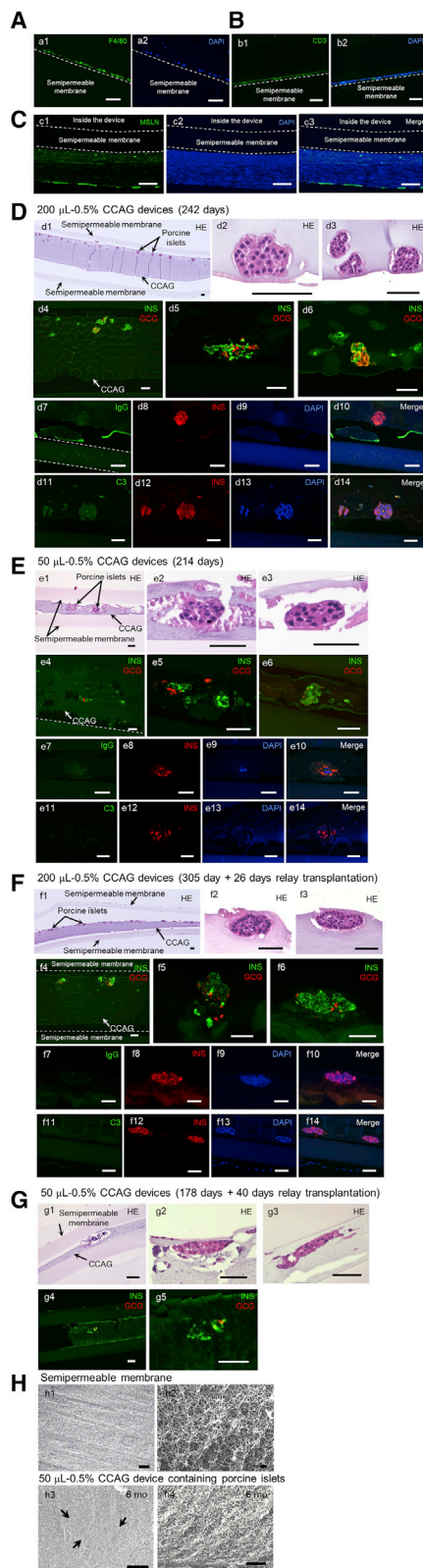
(A) Changes in non-fasting blood glucose levels in immunocompetent diabetic mice relay-transplanted with a device containing porcine islets. To verify that the transplanted devices could maintain their function for a long time, devices were retrieved at 22–396 days after transplantation and relay-transplanted into other immunocompetent wild-type diabetic mice. Porcine islet-containing devices with the crosslinked alginate gel were transplanted into immunocompetent diabetic mice. The devices were retrieved from mice with effective control of blood glucose levels and relay-transplanted into new immunocompetent diabetic mice for 1 month. The graph shows the blood glucose levels of all 31 relay-transplanted mice. Of the 31 transplanted mice, 16 exhibited blood glucose levels below 300 mg/dL for 1 month.

(B) The average non-fasting blood glucose levels of the 31 relay-transplanted mice.

(C) Kaplan-Meier curve of the rate of mice with an improved blood glucose level after relay-transplantation with a 50 μ L-0.5% CCAG device encapsulating porcine islets.

(D) Devices retrieved after relay-transplantation. The device was retrieved at 198 days after transplantation from an immunocompetent wild-type diabetic mouse and subsequently retrieved at 40 days after transplantation into a second immunocompetent wild-type diabetic mouse, panel 1 of (B). The device was retrieved at 178 days after transplantation from an immunocompetent wild-type diabetic mouse and then retrieved 40 days after transplantation into a second immunocompetent wild-type diabetic mouse, panels 2–4 of (B).

(E) Glucose-stimulated insulin secretion at 26–40 days after relay-transplantation into a second immunocompetent wild-type diabetic mouse. After transplantation into immunocompetent diabetic mice for 178–305 days, the devices were retrieved and transplanted into new immunocompetent wild-type diabetic mice. Glucose concentration-dependent insulin secretion was compared using a paired t test.



semipermeable membrane bags and intraperitoneally transplanted them into immunocompetent wild-type diabetic mice in this study. Some important results were obtained. First, long-term glycemic control was achieved in immunocompetent diabetic mice, despite discordant xenotransplantations without the use of immunosuppressants (Figures 3C and 3E). Furthermore, after relay-transplantation into a second diabetic mouse, the glycemic control was also improved (Figures 4A and 4B). Thus, our new device is unprecedented in its ability to resist discordant xenogeneic biological reactions twice. The reason for relay-transplantation in this study was not to reuse the graft, but to evaluate its function under the severe conditions of two transplantations. As shown in Figures 3I and 3J, the GSIS from 0.5% CCAG devices encapsulating 10,000 IEQ of porcine islets 178–214 days after transplantation was reduced to about 5% (1/20) compared with the GSIS from 50 μ L-0.5% CCAG devices encapsulating 10,000 IEQ of porcine islets before transplantation. This suggests that about 500 IEQ islets survived. The death of many porcine islets in the device early after transplantation to mice was expected, but the fact that the islets survived for a long time probably contributed substantially to the decrease in blood glucose levels. The device was able to be retrieved because no adhesion or fibrosis occurred in the abdominal cavity of the mice over an extended period of time. Therefore, it was possible to quantify the survival rate of porcine islets as insulin secretion from the whole device. In addition, unlike those from neonatal or juvenile porcine islets or pluripotent stem cells, adult porcine islets do not differentiate *in vivo* when transplanted. Hence, the amount of insulin secreted by individual islets does not increase and it will thus reflect the islet survival rate. However, it was difficult to quantify the amount of viable porcine islets in the device

Figure 5. Representative immunohistochemical and electron microscopy images of the devices

(A) A 6-day transplanted 0.5% CCAG device was stained with anti-F4/80 antibody and DAPI.
 (B) A 6-day transplanted 0.5% CCAG device was stained with anti-CD3 antibody and DAPI.
 (C) The thin film that formed on the surface of a 3-month transplanted 0.5% CCAG device was stained with anti-mesothelin antibody and DAPI.
 (D) H&E images of 200 μ L-0.5% CCAG device islets retrieved at 242 days after transplantation (panels 1–3). Immunostaining with anti-insulin and anti-glucagon antibodies (panels 4–6); anti-IgG and anti-insulin antibodies (panels 7–10); and anti-C3 and anti-insulin antibodies (panels 11–14).
 (E) H&E images of a 50 μ L-0.5% CCAG device retrieved 214 days after transplantation (panels 1–3). Immunostaining with anti-insulin and anti-glucagon antibodies (panels 4–6); anti-IgG and anti-insulin antibodies (panels 7–10); and anti-C3 and anti-insulin antibodies (panels 11–14).
 (F) H&E images of a 200 μ L-0.5% CCAG device retrieved on day 26 of relay-transplantation after an initial transplantation for 305 days (panels 1–3). Immunostaining with anti-insulin and anti-glucagon antibodies (panels 4–6); anti-IgG and anti-insulin antibodies (panels 7–10); and anti-C3 and anti-insulin antibodies (panels 11–14).
 (G) H&E images of a 50 μ L-0.5% CCAG device retrieved on day 40 by relay-transplantation after an initial transplantation for 178 days (panels 1–3). Immunostaining with anti-insulin and anti-glucagon antibodies (panels 4 and 5). Scale bar, 50 μ m.
 (H) SEM images of the devices. Surface (panel 1) and cross-section (panel 2) of the semipermeable membrane. Surface (panel 3) and cross-section (panel 4) of a 50 μ L-0.5% CCAG device transplanted into a diabetic mouse for 6 months. Scale bar, 1 μ m.

by histological evaluation or blood porcine insulin concentration. Although the insulin content of individual encapsulated islets retrieved from mice has been reported, it is difficult to fully retrieve intraperitoneal microcapsules and total insulin secretion in all capsules cannot be quantified.³⁵ This is another outstanding aspect of our device.

The second advantage of this device is that it elicits only minimal inflammatory responses. There are many reports of capsule and device fibrosis after inflammatory responses.^{36–40} In addition, xenotransplantation of 10,000 IEQ microencapsulated neonatal porcine islets into mice showed more severe cell infiltration and cell adhesion than empty capsules.⁴¹ Although alginate gel encapsulation has been reported to prevent xenograft rejection, hydrogels alone are still problematic in terms of strength and gradual dissolution over long periods of time.⁴² However, in the initial and even in the relay-transplantation, only thin transparent films formed around our devices, and there was no evident fibrotic tissue formation, granulation tissue formation, or adhesions. This property also facilitated the retrieval and replacement of the device. It was also found that if the film around the device is thin, the exchange of nutrients and oxygen can be sufficient, and the porcine islets can survive. Surprisingly, the device was completely wrapped in the film. However, it did not adhere to the surface of the cellulose membrane at all and could be peeled off smoothly.

The third advantage is that the device was isolated from the immune reaction. Immunohistochemical analysis revealed that no host cells invaded the devices, indicating that it can block cell-mediated immunity. The retrieved devices showed that IgG and C3 (Figures 5D–5G) had hardly invaded the devices, consistent with the *in vitro* results (Figures 2F and 2G). These findings suggest that the device can also protect against humoral immunity. However, other substances involved in immunity (e.g., cytokines, chemokines, nitric oxide) that are smaller than 100 kDa in weight are believed to permeate the devices^{32,33} and these substances cannot be blocked by membranes and gels alone. For the immunoprotective function of the device, it may be important that not only IgG and complements but also small-molecule cytokines, such as IFN- γ , IL-1 β , and TNF- α , do not diffuse into the device.⁴³ The invasion of cytokines has not been investigated this time, but it seems that further investigation is required.

Our data show that CCAGs are superior to NAGs and that highly stable CCAGs help to ensure that the devices are effective for long-term glycemic control. Furthermore, CCAGs had no adverse effect on cell survival, similar to NAGs, as evidenced by their good glycemic control effect. In addition, CCAG conditions comprising a lower gel concentration, lower induction rate of chemical crosslinking, and lower gel amount exhibited the most effective glycemic control in diabetic mice (Table 1). This is consistent with the results of the oxygen pressure simulation (Figures 2F and 2G). Oxygen pressure in the portal vein (a standard site of islet transplantation) has been reported to be approximately 40 mmHg.⁴⁴ However, the oxygen pressure in the transplanted islets themselves is very low at 5 mmHg.^{44–48} In contrast, our transplanted devices are estimated to be exposed intraperitoneally to an environment under oxygen pressure of approximately 30–40 mmHg.^{44,48,49} The oxygen concen-

tration in the central part of devices with 50- μ L alginate gel (thickness, 0.25 mm) would be 40%–50% of that outside the device (Figure 2F). Therefore, the central partial pressure of oxygen was predicted to be 16–20 mmHg, suggesting that the oxygen concentration is well above the lower limit for islet survival.

We have created macrodevices for islet transplantation using alginate gels and semipermeable membranes. However, multiple studies of devices for the treatment of T1D have been conducted. In these studies, chitosan gel and ethylene-vinyl alcohol devices that encapsulated rat pancreatic islets were transplanted intraperitoneally or subcutaneously into mice.^{50,51} The devices were observed only up to 1 month after transplantation, and it is unclear whether long-term function can be maintained. In addition, they involved concordant xenotransplantation in which rat pancreatic islets were transplanted into mice, and the immune response received by the devices differs from that of our transplantation of porcine pancreatic islets into mice, that is, discordant xenotransplantation. Treatment of T1D using xenogeneic islets requires the development of macrodevices that can avoid and resist the immune response of discordant xenotransplantation and maintain device function for a long period of time.

Although many studies of alginate gels combining derivatives and ion gelation have been reported,^{52–57} there are no studies in which the transplanted alginate gel device has functioned *in vivo* for a long period of time. However, studies have reported that ion-crosslinking azido alginate gels have high physical/chemical stability,^{52–54} show a low host immune response, and have few foreign reactions and minimal inflammation.⁵⁵ In addition, the ion-crosslinking azido alginate gel has good cellular compatibility between human and rat pancreatic islets⁵² and exhibits high biological activity in cell adhesion and cell proliferation assays.^{56,57} These results support the results of improved long-term transplant outcomes with our device.

In this study, 10,000 IEQ porcine islets were required to improve blood glucose levels in immunocompetent wild-type diabetes mice (Figure 5D). The large number of porcine islets required for xenotransplantation is due to the low transplant survival of porcine islets after transplantation, not the low insulin secretory capacity of porcine islets.^{58–60} In general, the number of islets required to improve blood glucose levels in mouse diabetes models is species dependent. In the case of subrenal capsule transplantation into immunocompromised mice, which is often used in experiments due to its relatively high viability, it has been reported that 100–200 islets are required for mouse islets^{61–63} and 500–2,000 islets for human islets,^{63–66} while porcine islets require significantly more islets, about 2,000–12,600 IEQ.^{67–74}

One of the reasons for the low survival rate is suggested to be the brittleness of porcine islets. It has been reported that, during the isolation process, porcine islets are isolated from exocrine cells and the basement membrane of the pancreas by collagenase, resulting in diverse sizes and heterogeneous morphology, and that porcine islets are particularly fragile.^{75–78} Therefore, porcine islets are assumed to show low survival. In contrast, when porcine islets are transplanted into monkey diabetes models or humans, efficacy has been observed at 10,000–20,000 IEQ/kg,^{11,12,79,80} which is higher than, but not

so different from, that of islet transplantation from human donors to humans (5,000–15,000 IEQ/kg). Although the mechanism has not been fully elucidated, there seems to be a large species difference. In conclusion, transplantation of porcine islets into diabetic mice generally requires many porcine islets. In addition, unlike subrenal capsule transplantation, device-encapsulated transplantation might require an even higher number of islets because of the distance from the blood vessels and the disadvantage in terms of oxygen supply. However, there might be an advantage for device transplantation in terms of the physical protection of fragile porcine islets by their encapsulation in alginate gel. We will consider dose optimization for chemically modified alginate gel devices once the device conditions are optimized.

For device sizes, one device (2 cm²) of this study contained 10,000 IEQ of porcine pancreatic islets. For the transplantation of 10,000 IEQ/kg into a human (weight, 60 kg), 60 devices would be required, giving a total calculated area of 120 cm². This is about the size of a postcard and therefore does not seem to be unrealizable. However, efforts to decrease the size even further are needed, by, for example, making the thickness of the gel more uniform, precisely arranging the islets so that the distance between them is constant, or placing the islets in two layers, front and back. In addition, if device improvements can reduce the loss of porcine islets after transplantation, the required transplantation amount can be further reduced. Mice transplanted with the device are clearly divided into cases where the blood glucose returns to hyperglycemia and cases where the blood glucose levels can be improved for a long period of time in the early stage after transplantation. The reason is still unknown. In addition, the reason why cellulose membranes are less likely to cause adhesions and inflammation is also unclear. We need to clarify the reason why the device does not cause a foreign body reaction or an immune reaction.

Limitations of the study

This study has some potential limitations. First, the device has been shown to be highly permeable to glucose, insulin, and oxygen under each device condition. However, it is less permeable than naked porcine islets due to the encapsulation of the porcine islets with alginate gel and cellulose membrane. Due to the property of the device itself, the insulin response might be delayed. This was not a major problem in mice but might be a problem in humans.

Second, a large number of porcine islets needs to be transplanted to improve blood glucose levels in diabetic mice for a long period of time. Many porcine islets die early after transplantation to mice. However, it is also true that a small number of porcine islets survive long term in the device. It would be useful to know the differences in characteristics and conditions between surviving and dead islets. Unfortunately, however, it is not yet possible to distinguish between islets that survive for a long time and islets that die early (e.g., size, shape, and other factors). To reduce the number of porcine islets to be transplanted, it is necessary to devise ways to eliminate the initial loss.

Third, although a mouse model was used in this study, if the devices need to be transplanted into the abdominal cavity of humans, risks not seen by transplantation into small animals, such

as mice, should be tested with particular care in large animals. One such risk is organ damage. We are considering experiments involving the xenotransplantation of porcine islet-containing devices into large animals and aim to develop devices that enable more efficient long-term cell survival without the use of immunosuppressants. It seems important to ensure that no foreign body reaction or cellular overgrowth is induced in various animals and in humans.^{37,38} This is a subject for future research.

Fourth, for fibrosis, the mechanistic reason why the device did not undergo strong fibrosis is not clear. The device bag used in this study is made of cellulose acetate. Although it is not used as a drug, it is used as a dialysis membrane for hemodialysis treatment and as a patch, and it is a material that exhibits enhanced biocompatibility via the reaction of cellulose with acetic acid and the acetylation of hydroxyl groups. Furthermore, the membrane has mechanical strength and there is no risk of dissolution, unlike with hydrogels. This device does not cause adhesion or severe fibrosis after implantation. However, a very soft and thin membrane is formed on the surface after transplantation. This thin film did not adhere to the device at all and peeled off easily without resistance. In other words, it seems to be different in nature from the fibrous tissue caused by the usual foreign body reaction. Importantly, this thin film does not interfere with permeability or small-molecule exchange, and the cells inside the device can survive. How it differs from conventional fibrous tissue is a future research topic.

Finally, only 2 of the 30 mice showed elevated blood glucose levels after device retrieval. In cases where blood glucose did not rise after removal, we speculate that pancreatic β cells might have regenerated in diabetic mice during the long-term observation period. This occurred at a higher rate than reported previously, but we speculate that the ability to avoid hyperglycemia for a very long period may effectively promote β cell regeneration. Another possibility is that living cells, such as porcine islets, may be producing some unknown factors to accelerate the β cell regeneration. Because the aim of this study was to evaluate the function of the porcine islet device, we did not pursue in depth the β cell regeneration in mice; instead, we proved that the grafts were functional after long-term relay-transplantation into another diabetic mouse.

We created a semipermeable membrane bag device in which porcine islets were encapsulated in a developed alginate gel and intraperitoneally transplanted into immunocompetent wild-type diabetic mice in this study. This device permitted long-term glycemic control without the need for immunosuppressants. Devices created using the developed CCAG, which achieved both good stability and permeability, exhibited maintained islet engraftment and glycemic control even after relay-transplantation. The device could prevent rejection without immunosuppressive drugs and can withstand discordant xenotransplantation twice. Our aim is to further improve the device for potential clinical application.

STAR★METHODS

Detailed methods are provided in the online version of this paper and include the following:

- **KEY RESOURCES TABLE**
- **RESOURCE AVAILABILITY**
 - Lead contact
 - Materials availability
 - Data and code availability
- **EXPERIMENTAL MODEL AND SUBJECT DETAILS**
 - Animal models
- **METHOD DETAILS**
 - Porcine islet isolation and device fabrication
 - Device production
 - Immunocompetent wild-type diabetic mice and xeno-transplantation
 - Alginate gel stability
 - Diffusion of glucose, insulin, and IgG
 - Complement isolation
 - Simulation of oxygen diffusion and insulin secretion
 - Mechanical strength of the cellulose membranes
 - Transplantation and retrieval of the devices
 - Relay-transplantation
 - Blood glucose level monitoring
 - Intraperitoneal glucose tolerance test
 - Kaplan–Meier survival curve
 - Porcine insulin in the blood serum of mice
 - Glucose-stimulated insulin secretion
 - Immunohistochemical analysis of the devices and surrounding tissues
 - Antibodies
 - Scanning electron microscopic analysis
- **QUANTIFICATION AND STATISTICAL ANALYSIS**

SUPPLEMENTAL INFORMATION

Supplemental information can be found online at <https://doi.org/10.1016/j.crmeth.2022.100370>.

ACKNOWLEDGMENTS

The authors would like to thank Dr. Kenji Kawai of the Central Institute for Experimental Animals for preparing the histological specimens. We also thank the staff of Mochida Pharmaceutical Co., Ltd., including Yukiko Yatagai, Aya Kawamura, Tomohiko Sato, Masaki Yano, Yuko Sukegawa, Akira Takahashi, and Akihiro Mizushima for technical assistance and general support. This research received no specific grant from any funding agency in the public, commercial, or not-for-profit sectors. This work was partially supported by research funds from Mochida Pharmaceutical Co., Ltd.

AUTHOR CONTRIBUTIONS

M.S., S.F., and S.M. were involved in the study design and data interpretation. K.A., N.T., T.T., S.F., S.M., K.S., Y.Y., S.A., C.O., and M.S. were involved in the data analysis. All authors critically revised the report, commented on drafts of the manuscript, approved the manuscript to be published, and agree to be accountable for all aspects of the work in ensuring that questions related to the accuracy or integrity of any part of the work are appropriately investigated and resolved.

DECLARATION OF INTERESTS

This work was partially supported by research funds from Mochida Pharmaceutical Co., Ltd. Sodium alginate was provided by Mochida Pharmaceutical Co., Ltd. M.S., S.F., and K.A. are inventors on Japan patent PCT/JP2020/025,324. This patent covers the synthesis of chemically modified sodium algi-

nate and the effectiveness of transplantation devices containing the alginate gels, which is also a topic of this manuscript.

Received: April 22, 2022

Revised: August 29, 2022

Accepted: November 23, 2022

Published: December 19, 2022

REFERENCES

1. Shapiro, A.M., Lakey, J.R., Ryan, E.A., Korbitt, G.S., Toth, E., Warnock, G.L., Kneteman, N.M., and Rajotte, R.V. (2000). Islet transplantation in seven patients with type 1 diabetes mellitus using a glucocorticoid-free immunosuppressive regimen. *N. Engl. J. Med.* 343, 230–238. <https://doi.org/10.1056/NEJM200007273430401>.
2. Ryan, E.A., Paty, B.W., Senior, P.A., Bigam, D., Alfadhli, E., Kneteman, N.M., Lakey, J.R.T., and Shapiro, A.M.J. (2005). Five-year follow-up after clinical islet transplantation. *Diabetes* 54, 2060–2069. <https://doi.org/10.2337/diabetes.54.7.2060>.
3. Hering, B.J., Clarke, W.R., Bridges, N.D., Eggerman, T.L., Alejandro, R., Bellin, M.D., Chaloner, K., Czarniecki, C.W., Goldstein, J.S., Hunsicker, L.G., et al. (2016). Clinical islet transplantation consortium, phase 3 trial of transplantation of human islets in type 1 diabetes complicated by severe hypoglycemia. *Diabetes Care* 39, 1230–1240. <https://doi.org/10.2337/dc15-1988>.
4. Groth, C.G., Korsgren, O., Tibell, A., Tollemar, J., Möller, E., Bolinder, J., Ostman, J., Reinholt, F.P., Hellerström, C., and Andersson, A. (1994). Transplantation of porcine fetal pancreas to diabetic patients. *Lancet* 344, 1402–1404. <https://doi.org/10.2337/dc15-1988>.
5. Wynyard, S., Nathu, D., Garkavenko, O., Denner, J., and Elliott, R. (2014). Microbiological safety of the first clinical pig islet xenotransplantation trial in New Zealand. *Xenotransplantation* 21, 309–323. <https://doi.org/10.1111/xen.12102>.
6. Matsumoto, S., Abalovich, A., Wechsler, C., Wynyard, S., and Elliott, R.B. (2016). Clinical benefit of islet xenotransplantation for the treatment of type 1 diabetes. *EBioMedicine* 12, 255–262. <https://doi.org/10.1016/j.ebiom.2016.08.034>.
7. Scobie, L., Galli, C., Gianello, P., Cozzi, E., and Schuurman, H.J. (2018). Cellular xenotransplantation of animal cells into people: benefits and risk. *Rev. Sci. Tech.* 37, 113–122. <https://doi.org/10.20506/rst.37.1.2744>.
8. Tibell, A., and Groth, C.G. (1998). No viral disease after xenotransplantation. *Nature* 392, 646. <https://doi.org/10.1038/33517>.
9. Denner, J. (2016). How active are porcine endogenous retroviruses (PERVs)? *Viruses* 8, 215. <https://doi.org/10.3390/v8080215>.
10. Morozov, V.A., Wynyard, S., Matsumoto, S., Abalovich, A., Denner, J., and Elliott, R. (2017). No PERV transmission during a clinical trial of pig islet cell transplantation. *Virus Res.* 227, 34–40. <https://doi.org/10.1016/j.virusres.2016.08.012>.
11. Cooper, D.K.C., Ezzelarab, M.B., Hara, H., Iwase, H., Lee, W., Wijkstrom, M., and Bottino, R. (2016). The pathobiology of pig-to-primate xenotransplantation: a historical review. *Xenotransplantation* 23, 83–105. <https://doi.org/10.1111/xen.12219>.
12. Zhang, X., Li, X., Yang, Z., Tao, K., Wang, Q., Dai, B., Qu, S., Peng, W., Zhang, H., Cooper, D.K.C., and Dou, K. (2019). A review of pig liver xenotransplantation: current problems and recent progress. *Xenotransplantation* 26, e12497. <https://doi.org/10.1111/xen.12497>.
13. Ezzelarab, M.B., Ekser, B., Azimzadeh, A., Lin, C.C., Zhao, Y., Rodriguez, R., Echeverri, G.J., Iwase, H., Long, C., Hara, H., et al. (2015). Systemic inflammation in xenograft recipients precedes activation of coagulation. *Xenotransplantation* 22, 32–47. <https://doi.org/10.1111/xen.12133>.
14. Samy, K.P., Martin, B.M., Turgeon, N.A., and Kirk, A.D. (2014). Islet cell xenotransplantation: a serious look toward the clinic. *Xenotransplantation* 21, 221–229. <https://doi.org/10.1111/xen.12095>.

15. Farina, M., Alexander, J.F., Thekkedath, U., Ferrari, M., and Grattoni, A. (2019). Cell encapsulation: overcoming barriers in cell transplantation in diabetes and beyond. *Adv. Drug Deliv. Rev.* 139, 92–115. <https://doi.org/10.1016/j.addr.2018.04.018>.
16. Facklam, A.L., Volpatti, L.R., and Anderson, D.G. (2020). Biomaterials for personalized cell therapy. *Adv. Mater.* 32, e1902005. <https://doi.org/10.1002/adma.201902005>.
17. Elliott, R.B., Escobar, L., Tan, P.L.J., Muzina, M., Zwain, S., and Buchanan, C. (2007). Live encapsulated porcine islets from a type 1 diabetic patient 9.5 yr after xenotransplantation. *Xenotransplantation* 14, 157–161. <https://doi.org/10.1111/j.1399-3089.2007.00384x>.
18. Dufrane, D., and Gianello, P. (2012). Macro- or microencapsulation of pig islets to cure type 1 diabetes. *World J. Gastroenterol.* 18, 6885–6893. <https://doi.org/10.3748/wjgv18.i47.6885>.
19. Matsumoto, S., Tan, P., Baker, J., Durbin, K., Tomiya, M., Azuma, K., Doi, M., and Elliott, R.B. (2014). Clinical porcine islet xenotransplantation under comprehensive regulation. *Transplant. Proc.* 46, 1992–1995. <https://doi.org/10.1016/j.transproceed.2014.06.008>.
20. Iacovacci, V., Ricotti, L., Menciassi, A., and Dario, P. (2016). The bioartificial pancreas (BAP): biological, chemical and engineering challenges. *Biochem. Pharmacol.* 100, 12–27. <https://doi.org/10.1016/j.bcp.2015.08.107>.
21. Ludwig, B., Reichel, A., Steffen, A., Zimmerman, B., Schally, A.V., Block, N.L., Colton, C.K., Ludwig, S., Kersting, S., Bonifacio, E., et al. (2013). Transplantation of human islets without immunosuppression. *Proc. Natl. Acad. Sci. USA* 110, 19054–19058. <https://doi.org/10.1073/pnas.1317561110>.
22. Carlsson, P.O., Espes, D., Sedigh, A., Rotem, A., Zimmerman, B., Grinberg, H., Goldman, T., Barkai, U., Avni, Y., Westermarck, G.T., et al. (2018). Transplantation of macroencapsulated human islets within the bioartificial pancreas β Air to patients with type 1 diabetes mellitus. *Am. J. Transplant.* 18, 1735–1744. <https://doi.org/10.1111/ajt.14642>.
23. Gabr, M.M., Zakaria, M.M., Refaie, A.F., Ismail, A.M., Khater, S.M., Ashamalla, S.A., Azzam, M.M., and Ghoneim, M.A. (2018). Insulin-producing cells from adult human bone marrow mesenchymal stromal cells could control chemically induced diabetes in dogs: a preliminary study. *Cell Transplant.* 27, 937–947. <https://doi.org/10.1177/0963689718759913>.
24. David, A., Day, J., and Shikanov, A. (2016). Immunoisolation to prevent tissue graft rejection: current knowledge and future use. *Exp. Biol. Med.* 241, 955–961. <https://doi.org/10.1177/1535370216647129>.
25. Boettler, T., Schneider, D., Cheng, Y., Kadoya, K., Brandon, E.P., Martinson, L., and von Herrath, M. (2016). Pancreatic tissue transplanted in TheraCyte encapsulation devices is protected and prevents hyperglycemia in a mouse model of immune-mediated diabetes. *Cell Transplant.* 25, 609–614. <https://doi.org/10.3727/096368915X688939>.
26. Ramzy, A., Thompson, D.M., Ward-Hartstonge, K.A., Ivison, S., Cook, L., Garcia, R.V., Loyal, J., Kim, P.T.W., Warnock, G.L., Levings, M.K., and Kieffer, T.J. (2021). Implanted pluripotent stem-cell-derived pancreatic endoderm cells secrete glucose-responsive C-peptide in patients with type 1 diabetes. *Cell Stem Cell* 28, 2047–2061.e5, e5. <https://doi.org/10.1016/j.stem.2021.10.003>.
27. Kriz, J., Vilik, G., Mazzuca, D.M., Toleikis, P.M., Foster, P.J., and White, D.J.G. (2012). A novel technique for the transplantation of pancreatic islets within a vascularized device into the greater omentum to achieve insulin independence. *Am. J. Surg.* 203, 793–797. <https://doi.org/10.1016/j.amjsurg.2011.02.009>.
28. Pepper, A.R., Pawlick, R., Gala-Lopez, B., MacGillivray, A., Mazzuca, D.M., White, D.J.G., Toleikis, P.M., and Shapiro, A.M.J. (2015). Diabetes is reversed in a murine model by marginal mass syngeneic islet transplantation using a subcutaneous cell pouch device. *Transplantation* 99, 2294–2300. <https://doi.org/10.1097/TP.0000000000000864>.
29. Suzuki, K., Bonner-Weir, S., Trivedi, N., Yoon, K.H., Hollister-Lock, J., Colton, C.K., and Weir, G.C. (1998). Function and survival of macroencapsulated syngeneic islets transplanted into streptozocin-diabetic mice. *Transplantation* 66, 21–28. <https://doi.org/10.1097/00007890-199807150-00004>.
30. Ludwig, B., and Ludwig, S. (2015). Transplantable bioartificial pancreas devices: current status and future prospects. *Langenbeck's Arch. Surg.* 400, 531–540. <https://doi.org/10.1007/s00423-015-1314-y>.
31. Dufrane, D., Goebbels, R.M., Fdilal, I., Guiot, Y., and Gianello, P. (2005). Impact of porcine islet size on cellular structure and engraftment after transplantation: adult versus young pigs. *Pancreas* 30, 138–147. <https://doi.org/10.1097/01.mpa.0000147083.625011.4e>.
32. Carlsson, P.O., Palm, F., Andersson, A., and Liss, P. (2001). Markedly decreased oxygen tension in transplanted rat pancreatic islets irrespective of the implantation site. *Diabetes* 50, 489–495. <https://doi.org/10.2337/diabetes.50.3.489>.
33. Jung, H.S., Ahn, Y.R., Oh, S.H., Kim, Y.S., No, H., Lee, M.K., and Kim, K.W. (2009). Enhancement of beta-cell regeneration by islet transplantation after partial pancreatectomy in mice. *Transplantation* 88, 354–359. <https://doi.org/10.1097/TP.0b013e3181b07a02>.
34. Grossman, E.J., Lee, D.D., Tao, J., Wilson, R.A., Park, S.Y., Bell, G.I., and Chong, A.S. (2010). Glycemic control promotes pancreatic beta-cell regeneration in streptozotocin-induced diabetic mice. *PLoS One* 5, e8749. <https://doi.org/10.1371/journal.pone.0008749>.
35. Mitchelson, F., Safley, S.A., Gordon, K., Weber, C.J., and Sambanis, A. (2021). Peritoneal dissolved oxygen and function of encapsulated adult porcine islets transplanted in streptozotocin diabetic mice. *Xenotransplantation* 28, e12673. <https://doi.org/10.1111/xen.12673>.
36. Lambert, N., Wesche, J., Petersen, P., Doser, M., Zschocke, P., Becker, H.D., and Ammon, H.P.T. (2005). Encapsulation of islets in rough surface, hydroxymethylated polysulfone capillaries stimulates VEGF release and promotes vascularization after transplantation. *Cell Transplant.* 14, 97–108. <https://doi.org/10.3727/000000005783983232>.
37. Elliott, R.B., Escobar, L., Tan, P.L.J., Garkavenko, O., Calafiore, R., Basta, P., Vasconcellos, A.V., Emerich, D.F., Thanos, C., and Bamba, C. (2005). Intraperitoneal alginate-encapsulated neonatal porcine islets in a placebo-controlled study with 16 diabetic cynomolgus primates. *Transplant. Proc.* 37, 3505–3508. <https://doi.org/10.1016/j.transproceed.2005.09.038>.
38. Bochenek, M.A., Veisheh, O., Vegas, A.J., McGarrigle, J.J., Qi, M., Marchese, E., Omami, M., Doloff, J.C., Mendoza-Elias, J., Nourmohammadzadeh, M., et al. (2018). Alginate encapsulation as long-term immune protection of allogeneic pancreatic islet cells transplanted into the omental bursa of macaques. *Nat. Biomed. Eng.* 2, 810–821. <https://doi.org/10.1038/s41551-018-0275-1>.
39. Liu, Q., Chiu, A., Wang, L.H., An, D., Zhong, M., Smink, A.M., de Haan, B.J., de Vos, P., Keane, K., Vegge, A., et al. (2019). Zwitterionically modified alginates mitigate cellular overgrowth for cell encapsulation. *Nat. Commun.* 10, 5262. <https://doi.org/10.1038/s41467-019-13238-7>.
40. Liu, W., Flanders, J.A., Wang, L.H., Liu, Q., Bowers, D.T., Wang, K., Chiu, A., Wang, X., Ernst, A.U., Shariati, K., et al. (2022). A safe, fibrosis-mitigating, and scalable encapsulation device supports long-term function of insulin-producing cells. *Small* 18, e2104899. <https://doi.org/10.1002/smll.202104899>.
41. Itoh, T., Hata, Y., Nishinakamura, H., Kumano, K., Takahashi, H., and Kodama, S. (2016). Islet-derived damage-associated molecular pattern molecule contributes to immune responses following microencapsulated neonatal porcine islet xenotransplantation in mice. *Xenotransplantation* 23, 393–404. <https://doi.org/10.1111/xen.12253>. *Epub 2016 Jul 15*.
42. Vegas, A.J., Veisheh, O., Gürtler, M., Millman, J.R., Pagliuca, F.W., Bader, A.R., Doloff, J.C., Li, J., Chen, M., Olejnik, K., et al. (2016). Long-term glycemic control using polymer-encapsulated human stem cell-derived beta cells in immune-competent mice. *Nat. Med.* 22, 306–311. <https://doi.org/10.1038/nm.4030>.
43. Wang, X., Maxwell, K.G., Wang, K., Bowers, D.T., Flanders, J.A., Liu, W., Wang, L.H., Liu, Q., Liu, C., Naji, A., et al. (2021). A nanofibrous encapsulation device for safe delivery of insulin-producing cells to treat type 1 diabetes. *Sci. Transl. Med.* 13, eabb4601. <https://doi.org/10.1126/scitranslmed.abb4601>.

44. Vériter, S., Gianello, P., and Dufrane, D. (2013). Bioengineered sites for islet cell transplantation. *Curr. Diab. Rep.* *13*, 745–755. <https://doi.org/10.1007/s11892-013-0412-x>.
45. Rodriguez-Brotons, A., Bietiger, W., Peronet, C., Magisson, J., Sookhar-eea, C., Langlois, A., Mura, C., Jeandidier, N., Pinget, M., Sigrist, S., and Maillard, E. (2016). Impact of pancreatic rat islet density on cell survival during hypoxia. *J. Diabetes Res.* *2016*, 3615286. <https://doi.org/10.1155/2016/3615286>.
46. Carlsson, P.O., Liss, P., Andersson, A., and Jansson, L. (1998). Measurements of oxygen tension in native and transplanted rat pancreatic islets. *Diabetes* *47*, 1027–1032. <https://doi.org/10.2337/diabetes.47.7.1027>.
47. Johnson, A.S., Fisher, R.J., Weir, G.C., and Colton, C.K. (2009). Oxygen consumption and diffusion in assemblages of respiring spheres: performance enhancement of a bioartificial pancreas. *Chem. Eng. Sci.* *64*, 4470–4487. <https://doi.org/10.1016/j.ces.2009.06.028>.
48. Zimmermann, U., Nöth, U., Gröhn, P., Jork, A., Ulrichs, K., Lutz, J., and Haase, A. (2000). Non-invasive evaluation of the location, the functional integrity and the oxygen supply of implants: ¹⁹F nuclear magnetic resonance imaging of perfluorocarbon-loaded Ba²⁺-alginate beads. *Artif. Cells Blood Substit. Immobil. Biotechnol.* *28*, 129–146. <https://doi.org/10.3109/10731190009118576>.
49. Bose, S., Volpatti, L.R., Thiono, D., Yesilyurt, V., McGladrigan, C., Tang, Y., Facklam, A., Wang, A., Jhunjhunwala, S., Veiseh, O., et al. (2020). A retrievable implant for the long-term encapsulation and survival of therapeutic xenogeneic cells. *Nat. Biomed. Eng.* *4*, 814–826. <https://doi.org/10.1038/s41551-020-0538-5>.
50. Yang, K.C., Yanai, G., Yang, S.Y., Canning, P., Satou, Y., Kawagoe, M., and Sumi, S. (2018). Low-adhesive ethylene vinyl alcohol-based packaging to xenogeneic islet encapsulation for type 1 diabetes treatment. *Bio-technol. Bioeng.* *115*, 2341–2355. <https://doi.org/10.1002/bit.26730>.
51. Yang, S.Y., Yang, K.C., and Sumi, S. (2020). Prevascularization-free primary subcutaneous transplantation of xenogeneic islets coencapsulated with hepatocyte growth factor. *Transplant. Direct* *6*, e620. <https://doi.org/10.1097/TXD.0000000000001078>.
52. Hall, K.K., Gattás-Asfura, K.M., and Stabler, C.L. (2011). Microencapsulation of islets within alginate/poly(ethylene glycol) gels cross-linked via Staudinger ligation. *Acta Biomater.* *7*, 614–624. <https://doi.org/10.1016/j.actbio.2010.07.016>.
53. Deng, Y., Shavandi, A., Okoro, O.V., and Nie, L. (2021). Alginate modification via click chemistry for biomedical applications. *Carbohydr. Polym.* *270*, 118360. <https://doi.org/10.1016/j.carbpol.2021.118360>.
54. Gattás-Asfura, K.M., and Stabler, C.L. (2009). Chemoselective cross-linking and functionalization of alginate via Staudinger ligation. *Biomacromolecules* *10*, 3122–3129. <https://doi.org/10.1021/bm900789a>.
55. Moody, C.T., Palvai, S., and Brudno, Y. (2020). Click cross-linking improves retention and targeting of refillable alginate depots. *Acta Biomater.* *112*, 112–121. <https://doi.org/10.1016/j.actbio.2020.05.033>.
56. Jain, E., Neal, S., Graf, H., Tan, X., Balasubramaniam, R., and Huebsch, N. (2021). Copper-free azide-alkyne cycloaddition for peptide modification of alginate hydrogels. *ACS Appl. Bio Mater.* *4*, 1229–1237. <https://doi.org/10.1021/acsabm.0c00976>.
57. Lueckgen, A., Garske, D.S., Ellinghaus, A., Desai, R.M., Stafford, A.G., Mooney, D.J., Duda, G.N., and Cipitria, A. (2018). Hydrolytically-degradable click-crosslinked alginate hydrogels. *Biomaterials* *181*, 189–198. <https://doi.org/10.1016/j.biomaterials.2018.07.031>.
58. Smith, K.E., Purvis, W.G., Davis, M.A., Min, C.G., Cooksey, A.M., Weber, C.S., Jandova, J., Price, N.D., Molano, D.S., Stanton, J.B., et al. (2018). In vitro characterization of neonatal, juvenile, and adult porcine islet oxygen demand, β -cell function, and transcriptomes. *Xenotransplantation* *25*, e12432. <https://doi.org/10.1111/xen.12432>.
59. Mueller, K.R., Balamurugan, A.N., Cline, G.W., Pongratz, R.L., Hooper, R.L., Weegman, B.P., Kitzmann, J.P., Taylor, M.J., Graham, M.L., Schuurman, H.J., and Papas, K.K. (2013). Differences in glucose-stimulated insulin secretion in vitro of islets from human, nonhuman primate, and porcine origin. *Xenotransplantation* *20*, 75–81. <https://doi.org/10.1111/xen.12022>.
60. Cosimi, S., Marchetti, P., Giannarelli, R., Masiello, P., Bombara, M., Carmellini, M., Mosca, F., Arvia, C., and Navalesi, R. (1994). Insulin release in response to glucose from isolated mouse, rat, porcine, bovine, and human pancreatic islets. *Transplant. Proc.* *26*, 3421–3422.
61. Estil Les, E., Téllez, N., Nacher, M., and Montanya, E. (2018). A model for human islet transplantation to immunodeficient streptozotocin-induced diabetic mice. *Cell Transplant.* *27*, 1684–1691, Epub 2018 Oct 1. <https://doi.org/10.1177/0963689718801006>.
62. Gao, J., Tian, L., Weng, G., O'Brien, T.D., Luo, J., and Guo, Z. (2011). Stimulating β -cell replication and improving islet graft function by AR231453, A GPR119 agonist. *Transplant. Proc.* *43*, 3217–3220. <https://doi.org/10.1016/j.transproceed.2011.10.021>.
63. Pepper, A.R., Bruni, A., Pawlick, R., Wink, J., Rafiei, Y., Gala-Lopez, B., Bral, M., Abualhassan, N., Kin, T., and Shapiro, A.M.J. (2017). Engraftment site and effectiveness of the Pan-caspase inhibitor F573 to improve engraftment in mouse and human islet transplantation in mice. *Transplantation* *101*, 2321–2329. <https://doi.org/10.1097/TP.0000000000001638>.
64. Komatsu, H., Salgado, M., Gonzalez, N., Medrano, L., Rawson, J., Omori, K., Qi, M., Al-Abdullah, I., Kandeel, F., and Mullen, Y. (2020). High fractions of large islets in human islet preparations detrimentally affect posttransplant outcomes in streptozotocin-induced diabetic immunodeficient mice. *Pancreas* *49*, 650–654. <https://doi.org/10.1097/MPA.0000000000001541>.
65. Salgado, M., Gonzalez, N., Medrano, L., Rawson, J., Omori, K., Qi, M., Al-Abdullah, I., Kandeel, F., Mullen, Y., and Komatsu, H. (2020). Semi-automated assessment of human islet viability predicts transplantation outcomes in a diabetic mouse model. *Cell Transplant.* *29*, 963689720919444. <https://doi.org/10.1177/0963689720919444>.
66. Lebreton, F., Bellofatto, K., Wassmer, C.H., Perez, L., Lavallard, V., Parnaud, G., Cottet-Dumoulin, D., Kerr-Conte, J., Pattou, F., Bosco, D., et al. (2020). Shielding islets with human amniotic epithelial cells enhances islet engraftment and revascularization in a murine diabetes model. *Am. J. Transplant.* *20*, 1551–1561, Epub 2020 Mar 6. <https://doi.org/10.1111/ajt.15812>.
67. Korbitt, G.S., Elliott, J.F., Ao, Z., Smith, D.K., Warnock, G.L., and Rajotte, R.V. (1996). Large scale isolation, growth, and function of porcine neonatal islet cells. *J. Clin. Invest.* *97*, 2119–2129. <https://doi.org/10.1172/JCI118649>.
68. Purich, K., Cai, H., Yang, B., Xu, Z., Tessier, A.G., Black, A., Hung, R.W., Boivin, E., Xu, B., Wu, P., et al. (2022). MRI monitoring of transplanted neonatal porcine islets labeled with polyvinylpyrrolidone-coated superparamagnetic iron oxide nanoparticles in a mouse model. *Xenotransplantation* *29*, e12720. <https://doi.org/10.1111/xen.12720>. Epub 2021 Nov 30.
69. Kuppan, P., Kelly, S., Seeberger, K., Castro, C., Rosko, M., Pepper, A.R., and Korbitt, G.S. (2022). Bioabsorption of subcutaneous nanofibrous scaffolds influences the engraftment and function of neonatal porcine islets. *Polymers* *14*, 1120. <https://doi.org/10.3390/polym14061120>.
70. Salama, B.F., Seeberger, K.L., and Korbitt, G.S. (2020). Fibrin supports subcutaneous neonatal porcine islet transplantation without the need for pre-vascularization. *Xenotransplantation* *27*, e12575. <https://doi.org/10.1111/xen.12575>.
71. Goto, M., Maeda, A., Elfman, L., Suling, K.M., Wood, J.C., Patience, C., Groth, C.G., and Wennberg, L. (2004). No transmission of porcine endogenous retrovirus after transplantation of adult porcine islets into diabetic nude mice and immunosuppressed rats. *Xenotransplantation* *11*, 340–346. <https://doi.org/10.1111/j.1399-3089.2004.00144.x>.
72. Cui, H., Tucker-Burden, C., Cauffiel, S.M.D., Barry, A.K., Iwakoshi, N.N., Weber, C.J., and Safley, S.A. (2009). Long-term metabolic control of autoimmune diabetes in spontaneously diabetic nonobese diabetic mice by nonvascularized microencapsulated adult porcine islets. *Transplantation* *88*, 160–169. <https://doi.org/10.1097/TP.0b013e3181abbfc1>.
73. Foster, J.L., Williams, G., Williams, L.J., and Tuch, B.E. (2007). Differentiation of transplanted microencapsulated fetal pancreatic cells.

- Transplantation 83, 1440–1448. <https://doi.org/10.1097/01.tp.0000264555.46417.7d>.
74. Tu, J., Khoury, P., Williams, L., and Tuch, B.E. (2004). Comparison of fetal porcine aggregates of purified beta-cells versus islet-like cell clusters as a treatment of diabetes. *Cell Transplant.* 13, 525–534. <https://doi.org/10.3727/000000004783983693>.
 75. Swanson, C.J., Olack, B.J., Goodnight, D., Zhang, L., and Mohanakumar, T. (2001). Improved methods for the isolation and purification of porcine islets. *Hum. Immunol.* 62, 739–749. [https://doi.org/10.1016/s0198-8859\(01\)00255-5](https://doi.org/10.1016/s0198-8859(01)00255-5).
 76. Kim, H.I., Lee, S.Y., Jin, S.M., Kim, K.S., Yu, J.E., Yeom, S.C., Yoon, T.W., Kim, J.H., Ha, J., Park, C.G., and Kim, S.J. (2009). Parameters for successful pig islet isolation as determined using 68 specific-pathogen-free miniature pigs. *Xenotransplantation* 16, 11–18. <https://doi.org/10.1111/j.1399-3089.2008.00504.x>.
 77. Kang, S., Park, H.S., Jo, A., Hong, S.H., Lee, H.N., Lee, Y.Y., Park, J.S., Jung, H.S., Chung, S.S., and Park, K.S. (2012). Endothelial progenitor cell cotransplantation enhances islet engraftment by rapid revascularization. *Diabetes* 61, 866–876. <https://doi.org/10.2337/db10-1492>.
 78. Haque, M.R., Jeong, J.H., and Byun, Y. (2016). Combination strategy of multi-layered surface camouflage using hyperbranched polyethylene glycol and immunosuppressive drugs for the prevention of immune reactions against transplanted porcine islets. *Biomaterials* 84, 144–156, Epub 2016 Jan 19. <https://doi.org/10.1016/j.biomaterials.2016.01.039>.
 79. Morozov, V.A., Wynyard, S., Matsumoto, S., Abalovich, A., Denner, J., and Elliott, R. (2017). No PERV transmission during a clinical trial of pig islet cell transplantation. *Virus Res.* 227, 34–40. <https://doi.org/10.1016/j.virusres.2016.08.012>.
 80. Holdcraft, R.W., Graham, M.J., Bemrose, M.A., Mutch, L.A., Martis, P.C., Janecek, J.L., Hall, R.D., Smith, B.H., and Gazda, L.S. (2022). Long-term efficacy and safety of porcine islet macrobeads in nonimmunosuppressed diabetic cynomolgus macaques. *Xenotransplantation* 29, e12747. <https://doi.org/10.1111/xen.12747>.
 81. Shinohara, K., Chujo, D., Tamura-Nakano, M., Kurokawa, T., Matsumoto, S., and Shimoda, M. (2021). High-quality porcine islets isolated from aged miniature pigs. *Xenotransplantation* 28, e12675. <https://doi.org/10.1111/xen.12675>.
 82. Shimoda, M., Noguchi, H., Fujita, Y., Takita, M., Ikemoto, T., Chujo, D., Naziruddin, B., Levy, M.F., Kobayashi, N., Grayburn, P.A., and Matsumoto, S. (2012). Improvement of porcine islet isolation by inhibition of trypsin activity during pancreas preservation and digestion using α 1-antitrypsin. *Cell Transplant.* 21, 465–471. <https://doi.org/10.3727/096368911X605376>.
 83. Buchwald, P. (2009). FEM-based oxygen consumption and cell viability models for avascular pancreatic islets. *Theor. Biol. Med. Model.* 6, 5. <https://doi.org/10.1186/1742-4682-6-5>.
 84. Dulong, J.L., and Legallais, C. (2007). A theoretical study of oxygen transfer including cell necrosis for the design of a bioartificial pancreas. *Bio-technol. Bioeng.* 96, 990–998. <https://doi.org/10.1002/bit.21140>.
 85. Dulong, J.L., Legallais, C., Darquy, S., and Reach, G. (2002). A novel model of solute transport in a hollow-fiber bioartificial pancreas based on a finite element method. *Biotechnol. Bioeng.* 78, 576–582. <https://doi.org/10.1002/bit.10230>.
 86. Dionne, K.E., Colton, C.K., and Yarmush, M.L. (1993). Effect of hypoxia on insulin secretion by isolated rat and canine islets of Langerhans. *Diabetes* 42, 12–21. <https://doi.org/10.2337/diab.42.1.12>.
 87. Iwata, H., Arima, Y., and Tsutsui, Y. (2018). Design of bioartificial pancreases from the standpoint of oxygen supply. *Artif. Organs* 42, E168–E185. <https://doi.org/10.1111/aor.13106>.
 88. Kawamoto, T. (2003). Use of a new adhesive film for the preparation of multi-purpose fresh-frozen sections from hard tissues, whole-animals, insects and plants. *Arch. Histol. Cytol.* 66, 123–143. <https://doi.org/10.1679/aohc.66.123>.

STAR★METHODS

KEY RESOURCES TABLE

REAGENT or RESOURCE	SOURCE	IDENTIFIER
Antibodies		
Guinea pig polyclonal anti-insulin antibody	Abcam	Cat#ab195956; RRID: AB_2877638
Rabbit polyclonal anti-glucagon antibody	ImmunoStar	Cat#20076; RRID: AB_572241
Rabbit mesothelin polyclonal antibody	Thermo Fisher Scientific	Cat#PA5-79698; RRID: AB_2746813
Rabbit monoclonal anti-CD3 antibody	Abcam	Cat#ab16669; RRID: AB_443425
Rabbit polyclonal anti-F4/80 antibody	Abcam	Cat#ab100790; RRID: AB_10675322
Rat monoclonal anti-C3 antibody	Abcam	Cat#ab11862; RRID: AB_2066623
Goat polyclonal anti-guinea pig IgG (H + L) secondary antibody labeled with CF TM 488A	Biotium	Cat#20017; RRID: AB_10559033
Goat polyclonal anti-guinea pig IgG (H + L) secondary antibody labeled with Alexa Fluor 647	Thermo Fisher Scientific	Cat#A-21450; RRID: AB_2735091
Goat polyclonal anti-rabbit IgG (H + L) cross-adsorbed secondary antibody Alexa Fluor Plus 647	Thermo Fisher Scientific	Cat#A32733; RRID: AB_2633282
Goat polyclonal anti-rat IgG (H + L) cross-adsorbed secondary antibody Alexa Fluor 488	Thermo Fisher Scientific	Cat#A-11006; RRID: AB_2534074
Goat anti-rabbit IgG (H + L) superclonal recombinant secondary antibody Alexa Fluor 488	Thermo Fisher Scientific	Cat#A27034; RRID: AB_2536097
Biological samples		
Fetal bovine serum	Biosera	Cat#FB-1003/500
Complement control	Denka Seiken Co., Ltd.	Cat#400376
Chemicals, peptides, and recombinant proteins		
Natural sodium alginate (SeaMatrix®)	Mochida Pharmaceutical Co., Ltd.	Cat#ALG100
Streptozotocin	Sigma-Aldrich	Cat#S0130
Medetomidine hydrochloride (DOMITOR®)	Nippon Zenyaku Kogyo Co., Ltd.	N/A
Midazolam (SANTOZ®)	Sandoz K.K.	N/A
Butorphanol tartrate (Vetorphale®)	Meiji Seika Pharma Co., Ltd	N/A
Isodine solution 10%	Mundipharma K.K.	N/A
Medium 199	Thermo Fisher Scientific	Cat#11043-023
Gentamicin sulfate (Gentacin®)	Takata Pharmaceutical Co., Ltd.	N/A
Atipamezole hydrochloride (Antisedan®)	Nippon Zenyaku Kogyo Co., Ltd.	N/A
Dithizone	Sigma-Aldrich	Cat#43820
Alginate lyase	Nippon Gene Co., Ltd.	Cat#319-08261
0.1% Tween 20	MP Biomedicals	Cat#103168
IgG-FITC	Sigma-Aldrich	Cat#F9636-1M
Collagen gel	Nippi Inc.	Cat#ASC-11-100-100PW
One-point CH50 buffer	Denka Seiken Co., Ltd.	Cat#400024
Brightase-C	Nippi Inc.	Cat#892432
Functionality/Viability solution	Corning	Cat#99-786-CV
10% formaldehyde solution	Fujifilm Wako Pure Chemical Corporation	Cat#16223-55
Neoprene W 0.5%	Nisshin EM Co., Ltd.	N/A
Carrazzi's Hematoxylin solution	Fujifilm Wako Pure Chemical Corporation	N/A
Eosin	Sakura Finetek Japan Co., Ltd.	N/A
Antigen retrieval buffer (100× Citrate Buffer pH 6.0)	Abcam	N/A
Blocking One Histo	Nacalai Tesque	Cat#06349-64
VECTASHIELD Vibrance Antifade Mounting Medium with DAPI	Vector Laboratories	Cat#H-1800

(Continued on next page)

Continued		
REAGENT or RESOURCE	SOURCE	IDENTIFIER
Critical commercial assays		
Semipermeable membranes (Biotech CE)	Repligen Corporation	MWCO 100 kDa
Glucose Assay Kit	BioAssay Systems	Cat#EBGL-100
Insulin Human ELISA Kit	Mercodia	Cat#10-1113-01
Porcine insulin ELISA kit	Mercodia	Cat#10-1200-01
Kawamoto's film method	Section-Lab Co., Ltd.	N/A
Experimental models: Organisms/strains		
C57BL/6Ncr mice	SLC Japan	10–12 weeks, male
Clawn miniature pig	Japan Farm CLAWN Institute	≥ 3 years old; ≥ 50 kg; n = 25; male and female
NIBS miniature pig	Nisseiken Co., Ltd.	≥ 3 years old; ≥ 50 kg; n = 25; male and female
Software and algorithms		
SPSS Statistics	IBM Corp.	Version 27
Other		
Glucose meter (Glutest Neo Alpha®)	Sanwa Kagaku Kenkyusho Co., Ltd.	N/A

RESOURCE AVAILABILITY

Lead contact

Further information and requests for resources and reagents should be directed to and will be fulfilled by the lead contact, Masayuki Shimoda (mshimoda@hosp.ncgm.go.jp).

Materials availability

There are restrictions to the availability of the chemically modified sodium alginate due to the patent (PCT/JP2020/025,324) of Mochida Pharmaceuticals Co., Ltd.

Data and code availability

- All data reported in this paper will be shared by the [lead contact](#) upon request.
- This paper does not report original code.
- Any additional information required to reanalyze the data reported in this paper is available from the [lead contact](#) upon request.

EXPERIMENTAL MODEL AND SUBJECT DETAILS

Animal models

All animal experiments were approved by the Institutional Review Board of the National Center for Global Health and Medicine (permission number: 21,013). Adult miniature pigs (≥ 3 years old; ≥ 50 kg; n = 25; male and female) were used as donors. All pigs were obtained from the Japan Farm CLAWN Institute (Clawn miniature pig; Kagoshima, Japan) and Nisseiken Co., Ltd. (NIBS miniature pig; Tokyo, Japan) and were transported to Narita Animal Science Institute (NAS Institute, Chiba, Japan) for breeding. Pig pancreata were removed as previously described⁸¹ at NAS Institute and transported to the National Center for Global Health and Medicine. Porcine islets were isolated by a modification of a previously described method.⁸¹ Porcine islets were purified and evaluated as described.^{81,82}

The obtained porcine islets were cultured at 37°C in a 5% CO₂ atmosphere overnight in Medium 199 (Thermo Fisher Scientific, Carlsbad, CA) supplemented with 10% heat-inactivated fetal bovine serum (Biosera, Kansas City, MO). After the overnight culture, the islet number was counted based on size (50–400 μm), and the obtained islet yield was calculated by converting the number of islets to the IEQ. Porcine islet viability was evaluated by the ratio of the number of fluorescein diacetate (FDA)-stained cells to the number of propidium iodide (PI)-stained cells in one islet, and a total of 50 islets was counted and averaged. Porcine islet purity was expressed as a percentage of the islets stained with dithizone (DTZ) to total pancreatic digestive tissue. Porcine islets with a purity of 70% or higher were used for bioartificial islet device production and transplantation.

METHOD DETAILS

Porcine islet isolation and device fabrication

Pancreata (Figure S4A) excised from adult pigs were treated with collagenase to obtain adult pig pancreatic islets (Figure 1B). Figure S4B is an image of isolated porcine islets stained with DTZ. The red-stained clusters indicate porcine islets, and the unstained cells are tissues other than endocrine cells, such as exocrine cells and adipocytes. Figure S4C shows FDA-stained living porcine islets, and Figure S4D shows PI-stained dead porcine islets in the same field of view. Most of the islet cells in the clusters were alive. Figure 1E is a bright-field image of porcine islets.

Device production

The tubular semipermeable membrane (MWCO 100 kDa, Biotech CE, Repligen Corporation, MA) was sealed on one side with a heat sealer (Fuji Impulse Co., Ltd., Chiba, Japan) and the other side was open. Porcine islets were dispersed in sodium alginate solutions. The suspension was placed in the bottom of an envelope-shaped semipermeable membrane with a micropipette. The enclosure was then folded to close it and sealed with a heat sealer. The sodium alginates in the devices were then gelled in CaCl_2 (55 mmol L^{-1}) solution or BaCl_2 solution (20 mmol L^{-1}) for 10 min and washed in saline for 10 min.

Two types of alginates were used: a natural sodium alginate (SeaMatrix, Mochida Pharmaceutical Co., Ltd., Tokyo, Japan) and a developed chemically modified sodium alginate (Figure 1C) in this study. The average molecular weight of natural sodium alginate is 170–180 kDa. It is an aqueous solution with a viscosity of approximately 100 mPa s in a 1% solution. M represents mannuronic acid and G represents guluronic acid, which are polysaccharides with a structure in which two kinds of uronic acids are linearly polymerized. Uronic acid has one carboxyl group and can be ion-crosslinked. Porcine islets dispersed in a 1.0% sodium alginate aqueous solution were gelled by barium ion crosslinking of 20 mmol L^{-1} BaCl_2 in a semipermeable membrane bag. In contrast, the chemically modified sodium alginate (Figure 1C, PCT/JP2020/025,324) was formed using covalent bonds between sodium alginate with 4-(2-aminoethoxy)-N-(3-azidopropyl) benzamide and sodium alginate with dibenzocyclooctyne-amine. The viscosity of chemically modified sodium alginate is 50–150 mPa s in a 1% solution.

Porcine islets were dispersed in a 0.5% or 1.0% mixed aqueous solution of sodium alginate containing 4-(2-aminoethoxy)-N-(3-azidopropyl) benzamide and sodium alginate containing dibenzocyclooctyne-amine. In the case of chemically modified alginic acid, the percentage of crosslinked groups introduced is shown as the “induction rate”, in which the total number of carboxyl groups in alginic acid is 100%. The induction rate was selected to be 2.3%–5.0% as long as the stability of the alginate gel was improved and the permeability of glucose and insulin could be maintained. They formed a CCAG comprising a covalent bond and calcium ion crosslinking in a semipermeable membrane bag.

Immunocompetent wild-type diabetic mice and xenotransplantation

Immunocompetent wild-type diabetic mice were used as recipients (Figure 1B). Male C57BL/6Ncr mice (10–12 weeks) were obtained from SLC Japan (Shizuoka, Japan). Mice were intraperitoneally injected with 145 mg/kg streptozotocin (STZ; Sigma-Aldrich, St. Louis, MO) in citrate buffer (pH 4.5) to induce diabetes. Mice whose blood glucose levels were confirmed to continuously be 300 or more and 600 mg/dL or less were used as a diabetes model for transplantation.

The prepared porcine islet-encapsulating alginate devices were transplanted into the abdominal cavities of 99 immunocompetent wild-type diabetes model mice without the use of immunosuppressants (Figure 1B). The transplanted devices comprised the following seven groups: 200 μL -1.0% NAG-containing semipermeable membrane devices transplanted into 30 mice; 200 μL -1.0% CCAG (induction rate, 5.0%)-containing semipermeable membrane devices transplanted into 7 mice; 200 μL -0.5% CCAG (induction rate, 5.0%)-containing semipermeable membrane devices transplanted into 11 mice; 100 μL -0.5% CCAG (induction rate, 5.0%)-containing semipermeable membrane devices transplanted into 7 mice; 200 μL -0.5% CCAG (induction rate, 2.3%)-containing semipermeable membrane devices transplanted into 10 mice; 100 μL -0.5% CCAG (induction rate, 2.3%)-containing semipermeable membrane devices transplanted into 13 mice; and 50 μL -0.5% CCAG (induction rate, 2.3%)-containing semipermeable membrane devices transplanted into 21 mice (Table 1). The transplanted devices retrieved from 31 of these mice were re-transplanted into the abdominal cavity of new diabetic mice (relay-transplantation) (panel 3 in Figure 1B).

Alginate gel stability

The mechanical strength of the alginate gel was evaluated *in vitro* by the degree of elution of sodium alginate into an aqueous solution. The natural sodium alginate and chemically modified sodium alginate were each dissolved in saline. The two types of chemically modified sodium alginate solutions were mixed in equal amounts immediately before use. These alginate solutions were rapidly enveloped in a semipermeable membrane bag ($24 \times 10 \text{ mm}$) and immersed in a 55 mmol L^{-1} CaCl_2 solution for 10 min to form a hydrogel. Chemically modified sodium alginate with an induction rate of 2.3% was used for the CCAGs. The alginate hydrogels were removed from the semipermeable membrane, and three pieces of the hydrogels were immersed in 12 mL saline and shaken at 37°C . The aqueous solution was collected over time. Upon completion of the testing, 12 μL of alginate lyase (319–08261, Nippon Gene Co., Ltd., Tokyo, Japan) was added to the test solution, which was then shaken overnight at 37°C to completely dissolve the hydrogel. The alginate concentration in the collected aqueous solution was measured by the carbazole-sulfuric acid method. Data are representative of three independent experiments and values are expressed as mean \pm SEM

Diffusion of glucose, insulin, and IgG

The substance permeability of the device for glucose, insulin, and IgG was evaluated *in vitro*. The glucose and insulin solutions comprised 250 μg glucose and 500 ng insulin in saline with 0.1% Tween 20 (103,168, MP Biomedicals, Irvine, CA). The IgG solution consisted of 250 μg IgG-FITC (F9636-1ML, Sigma-Aldrich) in saline with 0.1% Tween 20. Alginate solution was added to equal amounts of glucose, insulin, or IgG solution, which was then rapidly enveloped in a semipermeable membrane and immersed in a 55 mmol L^{-1} CaCl_2 solution for 10 min. The enveloped alginate hydrogel was immersed in 40 mL saline with 0.1% Tween 20 and stirred and the aqueous solution was collected over time. Glucose, insulin, and IgG-FITC concentrations in the collected aqueous solution were respectively measured with a Glucose Assay Kit (EBGL-100, BioAssay Systems, Hayward, CA), with an Insulin Human ELISA Kit (10-1113-01, Mercodia, Uppsala, Sweden), or by monitoring the fluorescence intensity with excitation/emission wavelengths of 485/535 nm. Data are representative of three independent experiments and values are expressed as mean \pm SEM

Complement isolation

To investigate the complement sequestration ability of the semipermeable membrane or alginate gel, the envelope-form semipermeable membrane and alginate gel-containing sensitized sheep erythrocyte solution was shaken in a physiological saline solution mixed with human serum. The hemolysis rate of the sheep erythrocytes was examined. Collagen gel (ASC-11-100-100PW, Nippi Inc., Tokyo, Japan) was used as a control. The natural sodium alginate, chemically modified sodium alginate, and collagen were each dissolved in One-point CH50 buffer (400,024, Denka Seiken Co., Ltd., Tokyo, Japan). A solution comprising 150 μL alginate solution with 50 μL sensitized sheep erythrocytes was enveloped in a semipermeable membrane (24 \times 10 mm) and immersed in a 55 mmol L^{-1} CaCl_2 solution for 10 min to form a hydrogel. Regarding collagen gelation, a solution comprising 150 μL chilled collagen solution with 50 μL sensitized sheep erythrocytes was enveloped in a semipermeable membrane (24 \times 10 mm) and immersed in saline at 37°C for 30 min. The hydrogel extracted from the semipermeable membrane was immersed in 3 mL saline with 10 μL complement control (400,376, Denka Seiken Co., Ltd.) and incubated at 30°C for 24 h. Upon completion of the testing, 1.5 μL of alginate lyase or Brightase-C (892,432, Nippi Inc.) was added to the test solution, which was then shaken at 37°C to completely dissolve the hydrogel. The hemolysis was measured by recording the absorbance intensity at 541 nm. Data are representative of three independent experiments and values are expressed as mean \pm SEM

Simulation of oxygen diffusion and insulin secretion

The relationship between the thickness of the device and the oxygen concentration inside the device or the amount of insulin secretion was simulated and evaluated. Oxygen diffusion and insulin secretion were calculated under the following conditions:

The oxygen consumption rate of islets was assumed to be constant, at $0.06 \times 10^{-12} \text{ mol s}^{-1} \cdot \text{IEQ}^{-1}$.⁸³ and uniform throughout the hydrogel, including the islets.

For convenience, the Bunsen solubility coefficient, α (the relationship between the oxygen concentration and oxygen tension), was assumed to be identical among different environments, such as the medium, tissue, and hydrogel, and was roughly estimated to be $1.45 \times 10^{-3} \text{ mol m}^{-3} \cdot \text{mmHg}^{-1}$.⁸⁴

The oxygen concentration of the hydrogel surface was assumed to be at a steady state at 6590 mg m^{-3} (142 mmHg) under normoxic conditions and 1860 mg m^{-3} (40 mmHg) in the peritoneal cavity.

In this simulation, we assumed that the semipermeable membrane allows oxygen to pass 100% freely and quickly, and the calculation was based only on the gel thickness.

Equation 1 is the diffusion equation for the oxygen concentration at steady state when the hydrogel was placed in the Cartesian coordinate system.

$$0 = D_{Ae} \left(\frac{\partial^2 C_{(x,y,z)}}{\partial x^2} + \frac{\partial^2 C_{(x,y,z)}}{\partial y^2} + \frac{\partial^2 C_{(x,y,z)}}{\partial z^2} \right) - r_{O_2} \quad (\text{Equation 1})$$

A diffusion coefficient D_{Ae} of $2.7 \cdot 10^{-9} \text{ m}^2 \cdot \text{s}^{-1}$.^{85,86} was used, and r_{O_2} was calculated from the islet number and the oxygen consumption rate. The x , y , and z directions were equally divided into $x = i\Delta$, $y = j\Delta$, and $z = k\Delta$ and the concentration was finite-differenced by the node value of $C(x, y, z) = C_{i,j,k}$, as shown in Equation 2:

$$C_{i,j,k} = \frac{1}{6} \left[C_{i-1,j,k} + C_{i+1,j,k} + C_{i,j+1,k} + C_{i,j-1,k} + C_{i,j,k+1} + C_{i,j,k-1} - \frac{\Delta^2 \cdot r_{O_2}}{D_{Ae}} \right] \quad (\text{Equation 2})$$

To simulate insulin secretion, oxygen concentration was converted to oxygen tension, pO_2 , using Equation 3:

$$C = \alpha \cdot pO_2 \quad (\text{Equation 3})$$

Insulin secretion was simulated using oxygen tension as previously described.⁸⁷ Briefly, second-phase insulin secretion, S_{pO_2} , was calculated using Equation 4:

$$\frac{S_{pO_2}}{S_{142}} = \frac{\left(\frac{pO_2}{16}\right)^2}{1 + \left(\frac{pO_2}{16}\right)^2} \quad (\text{Equation 4})$$

Mechanical strength of the cellulose membranes

The cellulose ester membrane was cut into a 35 × 6-mm dumbbell shape, shown in [Figure S5](#). Five specimens of each group were tested under uniaxial tensile load (Instron 5969, Norwich, MA) by pulling both ends of the membranes in water at a rate of 200 mm/min.

Transplantation and retrieval of the devices

STZ-induced diabetic mice were anesthetized by subcutaneous injection of a mixture of medetomidine hydrochloride (0.75 mg/kg; DOMITOR, Nippon Zenyaku Kogyo Co., Ltd., Fukushima, Japan), midazolam (4 mg/kg; SANTOZ, Sandoz K.K., Tokyo, Japan), and butorphanol tartrate (5 mg/kg; Vetorphale, Meiji Seika Pharma Co., Ltd., Tokyo, Japan). Their abdomens were then shaved and sterilized using 2% iodine (Mundipharma K.K., Tokyo, Japan), and an approximately 3-cm incision was made along the midline of the abdomen. The devices were washed with FBS-free M199 medium for 30 min and then with saline for 30 min before transplantation. They were transplanted into the intraperitoneal cavities of mice without fixation to tissue and without the use of immunosuppressants. Before the incision was closed, gentamicin sulfate (Gentacin, Takata Pharmaceutical Co., Ltd., Saitama, Japan) was intraperitoneally administered to prevent device contamination. The incision in the peritoneum was then closed using 5-0 nylon sutures and the skin was closed over the incision using wound clips. To awaken mice from anesthesia, atipamezole hydrochloride (0.75 mg/kg, Antisedan, Nippon Zenyaku Kogyo Co., Ltd.) was subcutaneously administered. The entire procedure was performed on a heating pad set to approximately 38°C. When the device was retrieved from the mouse, the animal was anesthetized in the same manner as for the transplant. After the abdomen incision, the device was retrieved from the abdominal cavity along with the tissue formed around the device to prevent bleeding.

Relay-transplantation

To investigate the efficacy of the devices retrieved from the mice, they were re-transplanted into new diabetic mice, and their effect on blood glucose levels was observed. As in the case of the first transplantation, only gentamicin was administered intraperitoneally, and no immunosuppressive or anti-inflammatory drug was used.

Blood glucose level monitoring

Non-fasting blood glucose levels were monitored two or three times a week following device transplantation. The blood glucose levels were measured using a glucose meter (Glutest Neo Alpha, Sanwa Kagaku Kenkyusho Co., Ltd., Aichi, Japan) with a measurement range of 0–600 mg/dL.

The conditions considered to indicate suppression of the rise in the blood glucose level were:

1. Blood glucose levels dropped to 300 mg/dL or less after transplantation.
2. Blood glucose levels were maintained below 300 mg/dL until device retrieval.
3. Blood glucose levels exceeded 300 mg/dL three or fewer times.

Intraperitoneal glucose tolerance test

To evaluate the efficacy of the devices transplanted into the diabetic mice, glucose (1.5 g/kg) was intraperitoneally administered after 6 h fasting and the blood glucose levels were monitored for 180 min. An intraperitoneal glucose tolerance test was performed for diabetic mice transplanted with porcine islet-encapsulating 200 μ L-1.0% NAG devices and porcine islet-encapsulating 50 μ L-0.5% CCAG devices, non-diabetic control mice without device transplantation, and diabetic mice without device transplantation. Data are representative of 6–10 independent experiments and values are expressed as mean \pm SEM

Kaplan–Meier survival curve

A Kaplan–Meier survival curve was compared by the log rank method with SPSS Statistics software (version 27; IBM Corp.). Differences between groups were analyzed using a log rank (Mantel-Cox) test. Statistical significance among three groups was set at a Bonferroni-adjusted $p < 0.017$. After device transplantation, all mice had blood glucose levels below 300 mg/dL. The total number of mice whose blood glucose level dropped to 300 mg/dL or less after transplantation—that is, the total number of transplanted mice—was set to 100%. Thereafter, the point at which blood glucose levels rose again was defined as the occurrence of an event. Mice that died while maintaining blood glucose levels of 300 mg/dL or less and mice from which the device had been retrieved were censored.

Porcine insulin in the blood serum of mice

Mouse serum was obtained by centrifugation of blood collected from the cheek of the mouse every 2 or 3 weeks after transplantation. Porcine insulin levels in the serum of device-transplanted mice were measured using a porcine insulin ELISA kit (Mercodia). The crossover rate between porcine insulin and mouse insulin is 0.3% or less.

Glucose-stimulated insulin secretion

To evaluate insulin secretion from porcine islet-encapsulating devices, we performed glucose-stimulated insulin secretion of the device before transplantation, of the device after retrieval from the first transplanted mice, and of the device after retrieval from relay-transplanted mice. After the devices were retrieved from the abdominal cavities of the mice, the thin films that formed around the devices were removed before the glucose-stimulated insulin secretion test was performed. The devices were sequentially incubated at 37°C in medium (Functionality/Viability solution, CMRL 1066 [-] glucose, Corning, NY) containing low glucose (2.8 mM) for 2 h after two 30-min washes in a low-glucose solution and then incubated in medium containing high glucose (25 mM) for 2 h, before finally being incubated in medium containing low glucose (2.8 mM) for 2 h after a 1-h wash. The secretion of porcine insulin from devices was measured using a porcine insulin ELISA kit (Mercodia). Data are representative of 18 independent experiments and values are expressed as mean \pm SEM

Immunohistochemical analysis of the devices and surrounding tissues

Devices retrieved from the abdominal cavities of the mice were evaluated histologically. After the devices were retrieved from the abdominal cavity of the mice, the thin film formed around the devices was removed if the glucose-stimulated insulin secretion test was to be performed. Therefore, the film was not adhered to the histological evaluation of the device in such cases. The retrieved devices were fixed in 10% formaldehyde solution (Fujifilm Wako Pure Chemical Corporation, Osaka, Japan). The samples were embedded in paraffin using an automatic paraffin-embedding device. Because the thin slices of the semipermeable membrane of the device easily peeled off from the slide glass and the thin slices of the alginate gel fragmented easily, paraffin sections were obtained at 3- μ m thickness using Kawamoto's film method (Section-Lab Co., Ltd., Hiroshima, Japan)⁸⁸ to prevent slice loss. In addition, the sections were placed on a glass slide coated with neoprene W 0.5% (Nisshin EM Co., Ltd., Tokyo, Japan) and then on a hot plate at 54°C to strengthen the adhesive force. The Kawamoto film was immersed in xylene at 60°C until it peeled off. The sections were then deparaffinized with xylene and ethanol. The deparaffinized slices were stained with hematoxylin (Carrazzi's Hematoxylin solution, Fujifilm Wako Pure Chemical Corporation) and eosin (Sakura Finetek Japan Co., Ltd., Tokyo, Japan) (H&E). The H&E-stained sections were observed with a fluorescence microscope (BZ-X710; Keyence Corporation, Osaka, Japan).

In addition, the devices were examined by immunohistochemistry for porcine insulin and glucagon, as well as mouse IgG and C3. The device and the surrounding tissues were stained with anti-F4/80 antibody, anti-CD3 antibody, and anti-mesothelin antibody.

For immunostaining with F4/80, CD3, and mesothelin, antigen retrieval was performed using an antigen retrieval buffer (100 \times Citrate Buffer pH 6.0; Abcam, Cambridge, UK) for 10 min at 95°C. For immunostaining with insulin, glucagon, IgG, and C3, antigen retrieval was not performed. Deparaffinized slices were blocked for 10 min at room temperature with Blocking One Histo (Nacalai Tesque, Kyoto, Japan). They were then incubated overnight with primary antibodies at a dilution of 1:100–400 at 4°C, followed by incubation with secondary antibodies at a dilution of 1:500 at room temperature for 1 h and protection from light. They were then mounted on glass slides with VECTASHIELD Vibrance Antifade Mounting Medium or VECTASHIELD Vibrance Antifade Mounting Medium with DAPI (Vector Laboratories, Burlingame, CA). Images were visualized under an all-in-one fluorescence microscope (BZ-X710) at 10 \times and 20 \times magnification.

Antibodies

Guinea pig polyclonal anti-insulin antibody was obtained from Abcam (ab195956) and used as primary antibody at a dilution of 1:400. Rabbit polyclonal anti-glucagon antibody was obtained from ImmunoStar (20,076; Hudson, WI) and used as primary antibody at a dilution of 1:400. Rabbit mesothelin polyclonal antibody was obtained from Thermo Fisher Scientific (PA5-79698) and used as primary antibody at a dilution of 1:100. Rabbit monoclonal anti-CD3 antibody was obtained from Abcam (ab16669) and used as primary antibody at a dilution of 1:100. Rabbit polyclonal anti-F4/80 antibody was obtained from Abcam (ab100790) and used as primary antibody at a dilution of 1:200. Rat monoclonal anti-C3 antibody was obtained from Abcam (ab11862) and used as primary antibody at a dilution of 1:100. Goat polyclonal anti-guinea pig IgG (H + L) secondary antibody labeled with CF 488A was obtained from Biotium (20,017; Fremont, CA) and used at a dilution of 1:500. Goat polyclonal anti-guinea pig IgG (H + L) secondary antibody labeled with Alexa Fluor 647 was obtained from Thermo Fisher Scientific (A-21450) and used at a dilution of 1:500. Goat polyclonal anti-rabbit IgG (H + L) cross-adsorbed secondary antibody Alexa Fluor Plus 647 was obtained from Thermo Fisher Scientific (A32733) and used at a dilution of 1:500. Goat polyclonal anti-rat IgG (H + L) cross-adsorbed secondary antibody Alexa Fluor 488 was obtained from Thermo Fisher Scientific (A-11006) and used at a dilution of 1:500. Goat anti-rabbit IgG (H + L) superclonal recombinant secondary antibody Alexa Fluor 488 was obtained from Thermo Fisher Scientific (A27034) and used at a dilution of 1:500.

Scanning electron microscopic analysis

The device was evaluated using an electron microscope before and after transplantation. Devices retrieved from the abdominal cavities of mice were fixed with 2% paraformaldehyde and 2% glutaraldehyde (in 30 mM HEPES buffer containing 100 mM NaCl and 2 mM CaCl₂) [pH 7.4] for 24 h at 4°C and washed with 30 mM HEPES buffer [pH 7.4]. Fixed samples were dehydrated in a graded ethanol series and immersed in *t*-butyl alcohol, frozen, and dried by a vacuum evaporator (JFD-20, JEOL, Tokyo, Japan). For membranes that were not transplanted into mice, phosphate buffered saline-soaked devices were washed with deionized distilled water, dehydrated in a graded ethanol series, and air-dried. These samples were coated with Pt using a magnetron sputter (MSP-1S, Vacuum Device, Ibaraki, Japan) and examined in a scanning electron microscope (IT-300, JEOL).

QUANTIFICATION AND STATISTICAL ANALYSIS

Data is presented as mean \pm SEM unless otherwise noted. A Kaplan–Meier survival curve was compared by the log rank method with SPSS Statistics software (version 27; IBM Corp.). Differences between groups were analyzed using a log rank (Mantel-Cox) test. Glucose concentration-dependent insulin secretion was compared using a paired *t*-test. Sample sizes, statistical analyses are reported in the figures, and p values are reported in the legends.